



AFRL-RW-EG-TP-2015-002

**Rapid Prototyping across the Spectrum:
RF to Optical 3D Electromagnetic
Structures**

**Jeffery W. Allen
Monica S. Allen
Brett R. Wenner**

**Air Force Research Laboratory
Munitions Directorate
Eglin AFB, FL 32542**

November 2015

Technical Paper

Period of Performance: February 2012 – December 2015

DISTRIBUTION A – Approved for public release; distribution unlimited. Approval confirmation # 96TW-2016-0091.

DESTRUCTION NOTICE: For unclassified, limited documents, destroy by any method that will prevent disclosure of contents or reconstruction of the document.

**AIR FORCE RESEARCH LABORATORY
MUNITIONS DIRECTORATE**

NOTICE AND SIGNATURE PAGE

Using Government drawings, specifications, or other data included in this document for any purpose other than Government procurement does not in any way obligate the U.S. Government. The fact that the Government formulated or supplied the drawings, specifications, or other data does not license the holder or any other person or corporation; or convey any rights or permission to manufacture, use, or sell any patented invention that may relate to them.

Qualified requestors may obtain copies of this report from the Defense Technical Information Center (DTIC) (<http://www.dtic.mil>).

AFRL-RW-EG-TP-2015-002 HAS BEEN REVIEWED FOR TECHNICAL CONTENT AND ASSESSED TO BE ACCURATE AND IS APPROVED FOR PUBLICATION IN ACCORDANCE WITH ASSIGNED DISTRIBUTION STATEMENT.

FOR THE DIRECTOR:

//SIGNED//

//SIGNED//

TIMOTHY KLAUSUTIS, PhD, DR-III
TERMINAL SEEKER SCIENCES
CTC LEAD

THOMAS LEWIS, DR-III
AFRL/RWWS PROGRAM MANAGER

This report is published in the interest of scientific and technical information exchange, and its publication does not constitute the Government's approval or disapproval of its ideas or findings.

REPORT DOCUMENTATION PAGE				<i>Form Approved OMB No. 0704-0188</i>	
The public reporting burden for this collection of information is estimated to average 1 hour per response, including the time for reviewing instructions, searching existing data sources, gathering and maintaining the data needed, and completing and reviewing the collection of information. Send comments regarding this burden estimate or any other aspect of this collection of information, including suggestions for reducing this burden, to Department of Defense, Washington Headquarters Services, Directorate for Information Operations and Reports (0704-0188), 1215 Jefferson Davis Highway, Suite 1204, Arlington, VA 22202-4302. Respondents should be aware that notwithstanding any other provision of law, no person shall be subject to any penalty for failing to comply with a collection of information if it does not display a currently valid OMB control number. PLEASE DO NOT RETURN YOUR FORM TO THE ABOVE ADDRESS.					
1. REPORT DATE (DD-MM-YY) 11-17-2015		2. REPORT TYPE Interim Report		3. DATES COVERED (From - To) Feb. 2012 – Dec. 2015	
4. TITLE AND SUBTITLE Rapid Prototyping across the Spectrum: RF to Optical 3D Electromagnetic Structures				5a. CONTRACT NUMBER N/A	
				5b. GRANT NUMBER N/A	
				5c. PROGRAM ELEMENT NUMBER 62602F	
6. AUTHOR(S) Jeffrey W. Allen Monica S. Allen Brett R. Wenner				5d. PROJECT NUMBER 20688404	
				5e. TASK NUMBER 001	
				5f. WORK UNIT NUMBER W02E	
7. PERFORMING ORGANIZATION NAME(S) AND ADDRESS(ES) Weapon Seeker Sciences Branch Weapon Engagement Division Air Force Research Laboratory, Munitions Directorate Eglin Air Force Base, FL 32542-6810 Air Force Materiel Command, United States Air Force				8. PERFORMING ORGANIZATION REPORT NUMBER	
9. SPONSORING/MONITORING AGENCY NAME(S) AND ADDRESS(ES) Air Force Research Laboratory Munitions Directorate Eglin Air Force Base, FL 32542-6810 Air Force Materiel Command United States Air Force				10. SPONSORING/MONITORING AGENCY ACRONYM(S) AFRL/RWWS	
				11. SPONSORING/MONITORING AGENCY REPORT NUMBER(S) AFRL-RW-EG-TP-2015-002	
12. DISTRIBUTION/AVAILABILITY STATEMENT Distribution A: Approved for public release; distribution unlimited. Approval confirmation # 96TW-2016-0091.					
13. SUPPLEMENTARY NOTES					
14. ABSTRACT One of the most important challenges faced by the DoD is agility on a changing battlefield. Many times we are only a step ahead of foes, and solutions presented to the warfighter need to address these rapidly evolving threats. This demands agile and rapid manufacturing and design which will enable open architectures that permit rapid prototyping; mission specific reconfigurability; material tailoring for specific applications; efficient small lot productions; better systems, faster and cheaper; modularity, complexity combined with flexibility, and a shortened supply chain. Additive manufacturing (AM) and 3D prototyping are a potential “game changer” and have important implications to the DoD as seen by the significant investment by the Federal government through initiatives such as NNMI (America Makes). Rapid prototyping can be seen as the seamless thread from design to manufacturing to maintainability that will enable rapid modernization for technological agility. AM technology has advanced considerably in the commercial sector with new materials like thermo-plastics, metals, and photopolymers that have been optimized for a specific additive process. But, much work is still needed to develop and optimize the materials and additive processes to adapt AM to demanding military applications. The challenge is not simply to apply existing AM techniques, but also to develop new materials, AM processes, design methods and corresponding intellectual property through demonstrations that show the utility and viability of AM based solutions specific to DoD needs. In this paper, we aim to develop a roadmap for 3D Rapid Prototyping of electromagnetic (EM) Structures and Devices. Pursuant to this goal, we perform a systematic review of the types of EM phenomena and applications, design methodology and various 3D rapid prototyping techniques used for such fabrication. We also look at some of the existing limitations of 3D rapid prototyping for EM applications and identify a roadmap where 3D rapid prototyping can bring disruptive advancements to the field.					
15. SUBJECT TERMS Electromagnetics, Rapid prototyping, Electromagnetic Engineered Materials, Effective Medium, Metamaterials					
16. SECURITY CLASSIFICATION OF:			17. LIMITATION OF ABSTRACT: SAR	18. NUMBER OF PAGES 43	19a. NAME OF RESPONSIBLE PERSON (Monitor) Jeffery W. Allen 19b. TELEPHONE NUMBER (Include Area Code) (850)-882-3559
a. REPORT Unclassified	b. ABSTRACT Unclassified	c. THIS PAGE Unclassified			

THIS PAGE INTENTIONALLY LEFT BLANK

TABLE OF CONTENTS

Section	Page
LIST OF FIGURES	vi
1. ABSTRACT.....	1
2. INTRODUCTION	1
3. PROGRESS HISTORY OF ENGINEERED EM MATERIALS.....	3
4. THEORETICAL METHODS TO DESIGN EM MEDIA/DEVICES.....	5
5. RAPID PROTOTYPING OF ELECTROMAGNETIC MEDIA DEVICES	10
5.1 Macroscaled features	11
5.2 Nanoscaled Features	16
5.3 Conformal Structures	23
6. CONCLUSIONS.....	26
7. ACKNOWLEDGMENTS	27
8. REFERENCES	27

LIST OF FIGURES

Figure	Page
Figure 1: Traditional forward flow for designing systems with desired function	2
Figure 2: Future flow for designing systems: reverse from traditional method	3
Figure 3: Depiction of the Transformation Optics (TO) methodology where (a) shows a field line in free space in Cartesian coordinates, and (b) shows the distorted field line with the coordinates distorted in the same fashion. A ray-tracing program has been used to calculate ray trajectories in the cloak, assuming that $R_2 \gg \lambda$. (c) and (d) show the classical electromagnetic cloak example where TO was applied to calculate the fields. (c) and (d) respectively show 2D cross section and 3D view of rays diverted within the annulus of cloaking material to emerge on the far side undeviated from their original course [41].	6
Figure 4: Examples of 3D metamaterial structures (a) Double-fishnet metamaterials, (b) Chiral metamaterials via stacked electron-beam lithography, (c) chiral metamaterials made via direct-laser writing and electroplating, (d) hyperbolic metamaterial, (e) metal-dielectric layered metamaterial composed of coupled plasmonic waveguides, (f) 3D split-ring resonators, (g) wide-angle visible negative-index metamaterial, (h) Connected cubic-symmetry negative-index metamaterial structure, (i) Metal cluster-of-clusters visible-frequency magnetic metamaterial, and (j) All-dielectric negative-index metamaterial composed of two sets of high-refractive index dielectric spheres arranged on a simple-cubic lattice [74].....	12
Figure 5: (a) Manufactured anisotropic metamaterial, (b) Measured dielectric tensor of material in (a) [8]	14
Figure 6: Examples of lenses fabricated with AM (a) GRIN lens fabricated using 3D printer. The fill factor decreases radially outwards and the voids are visible in the unit cells as you approach the periphery of the lens, (b) Results of 3D electromagnetic simulation of a homogenized 3D lens (with actual unit cells) carried out in HFSS: electric field shows focus at location of 25 cm, [29] (c) Experimental setup, the Luneberg lens is fed by an X-band waveguide mounted to the surface of the Luneberg lens, (d) Measured radiation pattern of the Luneberg lens at 10 GHz [83].....	15
Figure 7: Custom optical elements fabricated with 3D printing. Such elements embedded in interactive devices, opening up new possibilities for interaction including: unique display surfaces made from 3D printed light pipes (a) Novel internal illumination techniques, (b) custom optical sensors, (c) embedded optoelectronics, (d) Mechanical structure of an interactive device (similar to (c) [57], (e) 3D printed lenslets and printed optics, (f) Customized 3D printed lens array [84].....	16
Figure 8: Microscale lenses fabricated with two-photon lithography (a) SEM image of a fabricated conical lens with 80° apex (enlarged view in the inset), (b) SEM image of a fabricated conical lens with 120° apex angle (lateral view in the inset) [92] (c) SEM image of optical tweezers end facet, [93] (d) SEM image of miniaturized optical tweezers [94].....	17

Figure 9: SEM of 3D nanostructures: Insets present the corresponding computed optical intensity distributions. (a) 3D nanostructure patterned with mask 1 over a large area, limited only by the size of the mask, (b) (110) cross-sectional view of the structure in (a), (c) Top view of the same structure (red arrow points to an ~100-nm structure in width). Inset shows modeling (arrow indicates the direction of polarization of the exposure light). (d) (100) cross-sectional view of a 3D nanostructure formed with mask 1 and the filtered output of the 365-nm emission line from a conventional mercury lamp. The modeling (inset), which assumes perfect coherence, accounts accurately for the shape of this structure. (e) Structure generated with mask 2 and 355-nm light, (f) Structure generated from mask 2 with 514-nm laser light. The top layer of this structure, which is shown in the modeling, peeled off because of its thin connecting features to the underlying structure, (g) Structure generated with mask 3, (h) Close-up view of tilted (100) facet of this structure. The modeling in the inset corresponds to a cross-section cut through the middle of the pillars, (i) Magnified view of top surface of this structure; inset shows modeling results. (j) Bottom surface, inset shows modeling results. (k) Stack of sealed nano-channels made by using mask 4. The polarization direction is parallel to line (arrow), (l) Magnified cross-sectional view, inset shows modeling results [99]..... 18

Figure 10: 3D printed photonic crystals with defect lines (a) Large area SEM image of defect lines fabricated in holographic photonic crystal (PhC) template; (b) Enlarged view of SEM image of defect line in 3D PhC template; (c) Defect structures in UTPA letters are fabricated in 3D PhC template. The height of letters is 0.7 mm as designed in the motion stage control program [110] 19

Figure 11: Nanoparticle arrays fabricated using electron beam induced deposition (EBID) (a) SEM images of rod shaped Ag deposits created with a stigmated electron beam at dose of 50 pC [59], (b) A 4 x 4 square nanopillar array, developed by FIB, at the tip of a 50 nm gold coated multimode optical fiber. Each square has an edge dimension of 200 nm, (c) Nanopillars with an elliptical cross-section (d) Dimer nanopillars separated by ~ 18nm (e) Au nanopillars formed by FIB. SEM was taken at a 30 degree tilt (f) Pointed gold nanorods formed by employing FIB milling [112]..... 20

Figure 12: (a) and (b) Different views of a double loop nano-spiral, (c) Top view of a straight nanowire, (d) and (e) Lateral view of nanowires grown at 0° and 45° respectively, to the substrate plane, (f) Curved nanowire after magneto-optical Kerr effect measurements, The scale bar is 500 nm in all images, except in (c), where it is 100 nm [114]..... 21

Figure 13: 3D micro/nano structural SWCNT/polymer composites are fabricated by using two photon lithography. The structures shown are a (a) 8 μm long microbull, (b) micro teapot, (c) micro lizard, (d) nanowire suspended between two microboxes, (e) magnified image of (d) and (f) perspective view of the nanowire [115]..... 21

Figure 14: (a) Optical micrograph of standing U-shaped resonator (SUSR) arrays with different heights. The insets show FE-SEM micrographs of the SUSR unit in each array respectively [120]. (b) Oblique-view electron micrograph of a metamaterial structure fabricated by direct

laser writing and silver shadow evaporation that has been cut by a FIB to reveal its interior [121].
..... 22

Figure 15: (a) SEM image of array of parabolic reflectors coated with silver; (b) SEM image of single paraboloid; (c) plan view of single paraboloid with light transmission aperture visible at bottom center; and (d) close-up of light aperture etched with a focused ion beam [104] 22

Figure 16: (a) Conformal antenna patterned by sputtering [138], (b) Small spherical wire antenna covered with conductive paint [73], (c) Optical image of an antenna during the printing process [135]..... 24

Figure 17: Photograph of printed flexible metamaterial designed to operate in the THz range [119]..... 25

Figure 18: (a) Array of finished PIN diodes on a bent PET substrate [145], (b) and (c) shows transferred III-V InGaAsP quantum well heterostructure as the gain medium sandwiched between single layer Si photonic crystal membrane reflectors using multilayer stacked nanomembranes [146], (d) micrograph of 3x3 mm patterned nanomembrane transferred onto a 1x1” flexible PET substrate [148], (e) Image of fabricated photonic devices on Au coated PET substrate, (f) photo of a prototypical flexible optical link [149]..... 26

1. ABSTRACT

One of the most important challenges faced by the DoD is agility on a changing battlefield. Many times we are only a step ahead of foes, and solutions presented to the warfighter need to address these rapidly evolving threats. This demands agile and rapid manufacturing and design which will enable open architectures that permit rapid prototyping; mission specific reconfigurability; material tailoring for specific applications; efficient small lot productions; better systems, faster and cheaper; modularity, complexity combined with flexibility, and a shortened supply chain. Additive manufacturing (AM) and 3D prototyping are a potential “game changer” and have important implications to the DoD as seen by the significant investment by the Federal government through initiatives such as NNMI (America Makes). Rapid prototyping can be seen as the seamless thread from design to manufacturing to maintainability that will enable rapid modernization for technological agility. AM technology has advanced considerably in the commercial sector with new materials like thermo-plastics, metals, and photopolymers that have been optimized for a specific additive process. But, much work is still needed to develop and optimize the materials and additive processes to adapt AM to demanding military applications. The challenge is not simply to apply existing AM techniques, but also to develop new materials, AM processes, design methods and corresponding intellectual property through demonstrations that show the utility and viability of AM based solutions specific to DoD needs. In this paper, we aim to develop a roadmap for 3D Rapid Prototyping of electromagnetic (EM) Structures and Devices. Pursuant to this goal, we perform a systematic review of the types of EM phenomena and applications, design methodology and various 3D rapid prototyping techniques used for such fabrication. We also look at some of the existing limitations of 3D rapid prototyping for EM applications and identify a roadmap where 3D rapid prototyping can bring disruptive advancements to the field.

2. INTRODUCTION

Engineering design, development and manufacturing processes have evolved from bulky infrastructure built to deliver specific products to a much more flexible paradigm in recent years. This need is driven by shorter product lifecycles combined with diverse models and variants that are required to meet customer demands. This has resulted in manufacturing flexibility requirements that demand shorter development cycles with an emphasis on low cost (yet high quality) and repeatability over large quantities. An obvious example is the smart phone market where a new model is introduced every week with updated features and even new form and functionality. Thus, engineering considerations now include capacity to develop and introduce field-tested new products to the market quicker using existing facilities. This has prompted tremendous growth in the development of rapid prototyping and manufacturing processes [1, 2]. While most efforts have focused on the manufacturing aspects (mechanical form and function) of rapid prototyping, fewer have considered the potential that these new fabrication techniques have to develop specific materials and devices that are tailored to elicit the electromagnetic (EM) outputs required from a system [3].

Historically, device and systems engineering have followed a unidirectional transfer function (Figure 1) from the material properties that are available in nature to the system characteristics that can be derived from devices that are based on this limited set of materials. The flow can be thought of where the first stage is to choose models that describe the natural material (e.g.

crystallography). Next a model such as a Taylor series expansion or exciton model is developed to derive the material parameters of the media, and finally EM theory is applied to study the device characteristics like wave propagation, scattering, etc. that can be obtained from this material [4]. The devices are then integrated into a system to give an overall performance that is usually at least slightly different from the theoretically predicted characteristics since the limited range of available material parameters dictates the practically demonstrated outputs. The quest for understanding and controlling the material properties has focused on the properties of the bulk material which can be changed by altering the chemical structure or composition of a material. For example, alloys can provide mechanical strength; conductivity in semiconductors can be controlled using carrier concentration that can be varied using dopants. These efforts have contributed significantly to the progress of science through the accessibility to the range of materials available with varying electromagnetic, structural and mechanical properties. However, these efforts all assume a given atom or molecule, and that is the constraining limit.

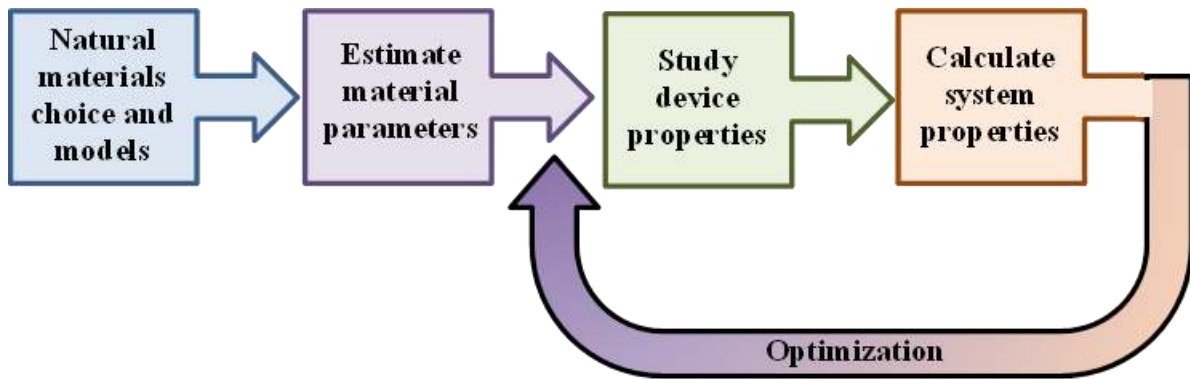


Figure 1: Traditional forward flow for designing systems with desired function

The ultimate goal would be to work in the reverse direction (Figure 2) where the system characteristics would determine the wave propagation and manipulation (e.g., negative group velocity, minimized scattering cross-section, etc.) needed from the material which in turn would derive the material parameters [5]. The final step in the process would be to develop experimental methods to synthesize the engineered medium using the calculated function. This approach would involve not limiting the scientist to the intrinsic chemical properties of the constituent materials where the fixed bonding structure determines the bulk properties that are then manipulated for device characteristics. Instead, artificial structures would be used to operate like atoms in a traditional material where the geometric and structural properties of these “atoms”, controlled through design, would determine the interaction with EM waves yielding physical properties and EM behavior that would be unattainable using naturally occurring or chemically synthesized materials [6].

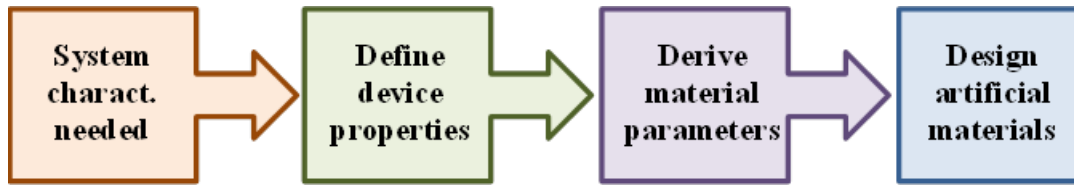


Figure 2: Future flow for designing systems: reverse from traditional method

In this review, we focus on theoretical methods and fabrication processes that can be used to design and practically implement complex EM structures. We begin with an overview of theoretical methods including analytical, optimization and transformation optics that can be used to design EM materials and devices to tailor the performance of the wave propagation or behavior needed for the application. Further, these methods can be used to define the exact geometric structure needed to realize the media and analyze how tolerant the defined media is to fabrication deviations. Next, we discuss the major fabrication methods that can be used to implement these materials and structures such that the features defined range from the macro- to the nano- scale and can be used in systems applied to operational wavelengths ranging from the radio frequency (RF)/microwave regime to the optical domain. We then discuss possible field applications, advantages of such a “bottom-up” method where the building blocks of matter can be defined and manipulated precisely to build larger systems rather than the traditional “top-down” methods where product construction is limited by the available intrinsic material parameters [6]. We conclude the article with future directions on both the design of new devices and media as well as suggestions for existing materials and fabrication techniques to improve the capabilities with respect to cost, size, weight and performance that are currently available.

3. PROGRESS HISTORY OF ENGINEERED EM MATERIALS

This review primarily deals with EM materials and devices. So what does EM response mean? It defines how an EM wave (composed of electric and magnetic fields) is affected as it impinges on and consequently reflects off and/or passes through and interacts with the given material or device. The two basic material parameters that lead to these effects are permittivity related to electric field interactions and permeability related to magnetic field responses. The electric and magnetic responses are mutually dependent as seen from Maxwell’s equations and can be spatially and temporally varied as well as nonlinear [7]. Conceptually, from an engineering perspective, one can think of the simple analogy where EM structures are to EM waves what circuits are to current and voltage. For example, a typical passive circuit offers control of the voltage and current of the supported guided modes. Similarly, EM structures can be used to manipulate incident and scattered waves in terms of direction and polarization as a function of space. Such control may allow the eventual implementation of arbitrary effective electric and magnetic current, and the physical manifestation of a Huygen source. There are several systems that rely on engineered EM devices and systems. These include functionality enabled by anisotropic or inhomogeneous media and metamaterials [8]. Specific examples of devices include antennas in the RF regime and photonic/electronic bandgap devices across frequency domains. Some of these devices and structures are discussed below.

The first area of application for these materials that has been explored in the context of EM engineered structures is small antenna design. Conventionally planar (2D) or wire (1D) antennas are employed which can be reduced in two dimensions at most; but, since they do not take into account volumetric considerations, these designs are not optimal for size reduction. 3D antennas that can fill or conform to arbitrary 3D shapes may provide the solution to maintaining/improving antenna performance while simultaneously reducing size [9]. 3D antenna designs with associated benefits were explored in detail by Chu [10], Wheeler [11] and Harrington [12] with refinement by Thal et al [13]. 3D antenna design can be broadly classified into (i) Conformal designs where the application limits the thickness of the antenna (e.g. antenna placed on aircraft fuselage need to be lightweight and aerodynamic); and (ii) 3D volumetric designs where the available cavity can be filled to desired thickness. In either case, careful consideration must be given to radiation pattern, gain, bandwidth, impedance and polarization, all of which directly impact the performance of the antenna or antenna array.

Complex EM structures are often composed of small physical features or individual constituents that are arranged in a periodic manner akin to atoms in a crystal lattice where individual cells interact with incident or propagating waves in a prescribed manner. One class of such periodic structures that has received much attention in the past is photonic bandgap (PBG) or electronic bandgap (EBG) structures [14, 15]. These periodic structures have been used to enable characteristics such as filtering including stop-bands, pass-bands, etc. Ideally, EBG devices are 3D periodic arrays of geometric structures that prevent the propagation of EM waves for a given frequency band at all incident angles independent of polarization. In practice, however, partial bandgaps are observed which cover limited incident angles [16].

Yet another area of application of these materials is inhomogeneous and/or anisotropic media. While some of these properties are commonly found in nature in the optical regime due to bandgaps that correspond to these wavelengths, the molecular resonances required to produce these effects at RF and microwave regimes are not found in nature [17]. Artificial materials can be designed to have spatially precise geometric properties that can be used to change the bulk material properties such as dispersion and anisotropy that can be effectively used to manipulate phase, polarization, wavefront and even time/phase symmetry [18]. Spatial variance of geometric features can be used to exploit directional phenomena and make the lattice structures inhomogeneous in the bulk material. Careful design is required to implement such macroscopic inhomogeneity so that the geometry of the individual unit cells that constitute the lattice is not deformed and the overall performance is maintained [5]. Traditionally, such designs are constructed using inherently lossy metals which limit their applicability in practical systems. Additionally, metals are not conducive to high power and high temperature applications due to concerns of excessive heating, changes in chemical reactivity, arcing, etc. Dielectric-only designs can be used to circumvent these issues, but typically designs based on these materials have weaker interaction with incident fields [8]. Therefore, the designs that have the requisite dispersion and anisotropy characteristics to produce the same behavior as their metallic counterparts are very complex and often have 3D geometries [19]. These structures are difficult to manufacture using conventional technologies such as planar printing of layers that are then stacked. Such structures find application in systems used for wavefront engineering, beam steering, devices, etc. [5]

The aforementioned structures are just some examples of the research and application areas for engineered EM materials. In past work, these structures have been fabricated using metal-dielectric layers where the features are defined using focused ion beam milling (e.g. fishnet patterns) [20], standard micro-/nano- lithography processes that are based on optical or electron beams. Most of these processes pattern single planar layers that then have to be stacked using sophisticated alignment techniques to produce 3D EM structures [21]. Thus the fabrication of truly 3D media is difficult and time-consuming and especially challenging in the optical regime where precise patterning and alignment of nanoscale features is needed [22].

Additive manufacturing processes such as 3D printing of macroscale features and multi-photon lithography for nanoscale attributes have been extensively researched in the context of rapid prototyping and manufacturing for a wide range of industries such as defense, medical, automotive and aerospace [23, 24]. Lesser emphasis has been laid on utilizing these techniques for building EM devices and structures. Recently, the field of engineered EM complexes has received much attention with the constant demand for lighter, cheaper, and faster turnaround technology. Several reports have documented the use of additive manufacturing to fabricate 3D EM devices, including gradient index lenses [25, 26] at both microwave [27, 28] and optical frequencies [26], and radio frequency lenses that attain resolution beyond the diffraction limit [29, 30]. These methods may be utilized to construct 3D EM designs [31, 32] that incorporate non-planar geometries and material inhomogeneity [33]. The entire process of designing, fabricating and characterizing these devices and structures is discussed in the next sections along with recent examples of applications of such media in practical systems.

4. THEORETICAL METHODS TO DESIGN EM MEDIA/DEVICES

Engineered materials and artificially constructed structures considered in this paper are analyzed by electrical, optical and RF engineers using EM field theory and models derived from it. The responses derived from these models can be then fed back into analytical, optimization and other design methods such as transformation optics to tailor the response of the designed media to the application. Two dominant phenomena that are considered in most of the models are: (i) Spatial dispersion: This results from the effect of neighboring point such as adjacent structures on a given point in a material. This directly influences the material polarization giving rise to a non-localized EM response such that the medium response varies with the direction of propagating waves; and (ii) Temporal dispersion: This describes the frequency dependence of wave-matter interaction and shows that the response of a medium at a specified point in time depends not only on the properties of the incident radiation at that time but also on past points. Both effects have been used to design and demonstrate interesting media such as chiral engineered and artificial magnetic materials[34]. While several simulation tools such as finite element method and finite difference time domain methods can be used to model the response and design such structures, we focus on the basic methods that are used within these models. They can be broadly classified as transformation optics design, analytical methods, and optimization techniques.

A popular method that can be used to design artificial EM materials is transformation optics (TO). While this method has been primarily used in the context of metamaterials, the basic concepts can be easily translated to the design of other artificial materials that enable the control of EM waves [35]. TO is a design methodology that allows control of wave propagation by accurately designing EM properties (permittivity and permeability) that define the space within which EM waves travel [36, 37]. An engineered EM device or media can be visualized using TO

by warping space so that waves propagate along a predefined path determined by the local metric [38, 39]. The warped space is related to the original/real space by a coordinate transformation (Figure 3). Since Maxwell's equations are form-invariant under a geometric coordinate transformation, it is simply a renormalization of the permittivity and permeability tensors that specify the EM material properties of the designed medium [40-42]. Numerous publications exist on using the TO method to transform passive space to demonstrate interesting devices such as cloaks, beam shifters and concentrators [41, 42]. Recently this methodology has been researched in the context of spaces that contain current or charge sources (e.g. generation/detection of electromagnetic waves). Such designs could enable practical devices such as arbitrary shaped antennas that radiate as if they were shaped differently like simple dipoles [43-45]. This would allow an engineer to consider mechanical form without compromising EM performance. While theoretically TO yields devices with very interesting behavior, experimental demonstrations of TO-based devices has been challenging since most of these transforms results in highly anisotropic material properties that vary continuously over a wide range of values. Practical fabrication techniques require these continuous material values be discretized. One method that has been used to demonstrate viable laboratory prototypes of media designed with TO is optimization. In the particular example of the cloak, optimization has been shown to not only give simpler material parameters using homogenous shells but also better performance [46].

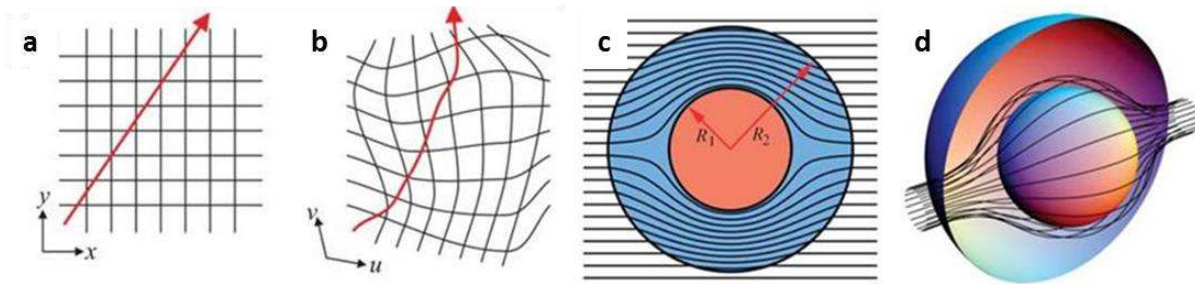


Figure 3: Depiction of the Transformation Optics (TO) methodology where (a) shows a field line in free space in Cartesian coordinates, and (b) shows the distorted field line with the coordinates distorted in the same fashion. A ray-tracing program has been used to calculate ray trajectories in the cloak, assuming that $R_2 \gg \lambda$. (c) and (d) show the classical electromagnetic cloak example where TO was applied to calculate the fields. (c) and, (d) respectively show 2D cross section and 3D view of rays diverted within the annulus of cloaking material to emerge on the far side undeviated from their original course [41].

Simple numerical optimization techniques have been widely applied to a variety of science and engineering problems and are most effective with a well-defined objective function that seeks maximum/minimum over a limited parameter space using a set of constraints [47, 48]. Ideally, the algorithm finds a global optimum and the problem is considered solved. However, a theoretically optimum solution may not be the most robust or stable [49]. Fabrication tolerances and deviations can adversely affect the device performance and thus a pareto front solution, that may not have the best performance but is more stable with parameter uncertainty, may hold the key to physically viable implementations [50]. These techniques have been explored in the context of antenna and antenna arrays as well as micro-/sub-millimeter wave components. In

these practical design applications, it is not uncommon to deal with multi-objective functions where the goals may be conflicting and a tradeoff must be made to strike a balance. In such cases, global optimization computational methods such as genetic algorithms and particle swarm optimization can be considered [28]. For example, in filter design, the optimization function is multi-objective and is a weighted sum that balances bandwidth, ripple and rejection ratio.

Once the device/media is designed, the next task is to characterize, model and predict the behavior of the designed structures. Several methods have been applied to the understanding of artificial engineered devices and media [51] with the most basic being the same methods used for designing EM structures and arrays such as transmission line theory and EM field theory [52]. Periodic media that are resonant structures can be analyzed using transmission line theory where the material properties including permittivity, permeability and refractive index can be modeled using the “LC” resonances which also determine the polarizability of the material [53]. The overall bulk material properties of a complex EM medium, made up of constitutive element whose parameters are controlled through careful geometric design, can be derived using homogenization methods. In addition, analytical models for polarizability of antenna structures have been widely explored [54]. These models can be applied to study bianisotropic, nonlinear and other complex materials [55]. Numerical methods like method of moments are applied to solve these formulations.

In complex EM materials, the material properties are derived from closely spaced electrically small constituent elements with minimal spatial dispersion. In such materials with specific engineered geometrical, mechanical, and EM properties, the focus is on deriving the constitutive tensor description of the material properties that define their overall behavior. To that end, constituent elements should be electrically small: the elements and inter-element spacing have to be small with respect to the propagating wavelengths in the corresponding directions within the effective medium. For equivalent materials with no propagating waves in particular directions (anisotropic/indefinite), the elements should be small with respect to the free-space wavelength. In order to be effectively applied in devices and systems, the material has to be characterized by constitutive tensors such that in a simulation and modeling scenario, if the EM material is replaced by the equivalent material with the appropriate constitutive tensor, the performance is comparable. The goal is to be able to use the macroscopic description of the material and apply it to describe the cumulative electromagnetic behavior of the material using Maxwell’s equations shown below:

$$\begin{aligned}\nabla \times \bar{H} &= \frac{\partial \bar{D}}{\partial t} + \bar{J}, \nabla \cdot \bar{B} = 0, \bar{B} = \bar{\mu} \bullet \bar{H} \\ \nabla \times \bar{E} &= -\frac{\partial \bar{B}}{\partial t}, \nabla \cdot \bar{D} = \rho, \bar{D} = \bar{\varepsilon} \bullet \bar{E}\end{aligned}$$

where $\bar{\mu}$ and $\bar{\varepsilon}$ represent the constitutive parameters, i.e. permeability and permittivity respectively. Various mixing models have been developed to solve the effective dielectric parameters of composites. These historical models are based on effective medium theory and continue to be widely used today. With the advent of precise control of material parameters through improved fabrication processes, these methods are attracting much interest in new applications such as metamaterials and engineered complex media. In these applications, digital control of material properties can be implemented using fabrication methods such as additive manufacturing techniques. In this context, mixing formulas and constitutive parameter retrieval

provide insight into how bottom-up design via geometrical and material property manipulation can be used to control material parameters with much greater flexibility than previously possible. It should be noted that the effective permittivity and permeability is different from the host medium as well as the electrically small inclusions. This can be primarily attributed to scattering which results in the average electric and magnetic fluxes being different from the properties of the host medium when it does not have any inclusions. There are several methods to derive the effective constitutive parameters. We will limit the examples to those where the unit cells can be reasonably defined.

Consider a classical mixing case with spheres in a host medium. For a volume scattering medium containing n spheres per unit volume, the polarization vector is related to the exciting field by $\bar{P} = n\alpha\bar{E}_e$, where \bar{E}_e is the exciting field and α is the polarizability of the sphere. One can thus arrive at the Clausius-Mossotti relation: $\varepsilon_{eff} = \varepsilon \left[\frac{1+2n\alpha/3\varepsilon}{1-n\alpha/3\varepsilon} \right]$ where ε is the background permittivity. Casting it in a symmetric form, we have:

$$\frac{\varepsilon_{eff} - \varepsilon}{\varepsilon_{eff} + 2\varepsilon} = fS = f \frac{\varepsilon_s - \varepsilon}{\varepsilon_s + 2\varepsilon}$$

where f is the fractional volume, ε_s is the permittivity of the sphere.

While this approach is very effective in the majority of complex materials, in some cases, the mixing formula can introduce unwanted resonances. This is especially obvious when the background medium consists of plasma with frequency below the plasma frequency and the inclusion is a lossless medium with positive real permittivity. When the fractional volume is small, the Bruggeman formula can provide more insight:

$$f_1 \frac{\varepsilon_1 - \varepsilon_{eff}}{\varepsilon_1 + 2\varepsilon_{eff}} + f_2 \frac{\varepsilon_2 - \varepsilon_{eff}}{\varepsilon_2 + 2\varepsilon_{eff}} = 0$$

Where $f_1 + f_2 = 1$, and $\varepsilon_1, \varepsilon_2$ are the corresponding permittivity values of the constituent materials. The permeability of the effective medium can be calculated similarly. Although these formulas are not universally applicable, they provide a simple mathematical basis for engineered digital EM materials and are useful for simple inclusions such as spheres, where the geometry of the inclusions is isotropic.

In many EM materials, irregularly shaped inclusions such as the split ring resonators are used. When the periodicity of the unit cells forms a simple non-overlapping lattice structure such as a tetragonal quasi-crystalline structure, numerical methods such as field averaging can be used to determine the effective material parameters. Consider a cubic lattice starting at the origin with period p as a special case of the tetragonal quasi-crystalline structure. Discretizing the frequency domain Maxwell's equations with time convention $e^{-i\omega t}$ such that

$$\begin{aligned} \nabla \times \bar{H} &= -i\omega\bar{D} \\ \nabla \times \bar{E} &= i\omega\bar{B} \end{aligned}$$

are applied to each sampled grid cell with size, for the D_x and B_y components, we have

$$\begin{aligned}\frac{\partial}{\partial y} H_z - \frac{\partial}{\partial z} H_y &= -i\omega D_x \\ \frac{\partial}{\partial z} E_x - \frac{\partial}{\partial x} E_z &= i\omega B_y\end{aligned}$$

Consider an Eigen-solution with the wave vector in the z direction, the electric field and flux in the x direction, and the magnetic field and flux in the y direction. Applying Stoke's theorem and integrating over the surface of the first unit cell for the electric and magnetic flux on the yz and xy plane respectively, we have

$$\begin{aligned}\int_0^p dy [H_y(0, y, d) - H_y(0, y, 0)] &= -i\omega p^2 D_{x,avg}(0, \frac{p}{2}, \frac{p}{2}) \\ \int_0^p dx [E_x(x, 0, d) - E_x(x, 0, 0)] &= i\omega p^2 B_{y,avg}(\frac{p}{2}, 0, \frac{p}{2})\end{aligned}$$

The co-located averaged electric and magnetic fields can be calculated based on:

$$\begin{aligned}E_{x,avg}(0, \frac{p}{2}, \frac{p}{2}) &= \frac{1}{p} \int_{-\frac{p}{2}}^{\frac{p}{2}} dx \left[E_x(x, \frac{p}{2}, \frac{p}{2}) \right] \\ B_{y,avg}(\frac{p}{2}, 0, \frac{p}{2}) &= \frac{1}{p} \int_{-\frac{p}{2}}^{\frac{p}{2}} dx \left[B_y(\frac{p}{2}, y, \frac{p}{2}) \right]\end{aligned}$$

The permittivity and the permeability in the x and y directions can be found from the ratio of the co-located averaged flux and averaged fields:

$$\begin{aligned}\epsilon_x &= \frac{D_{x,avg}(\frac{p}{2}, 0, \frac{p}{2})}{E_{x,avg}(\frac{p}{2}, 0, \frac{p}{2})} \\ \mu_y &= \frac{B_{y,avg}(0, \frac{p}{2}, \frac{p}{2})}{H_{y,avg}(0, \frac{p}{2}, \frac{p}{2})}\end{aligned}$$

Conversely, one can retrieve the medium parameters based on numerical simulations or measurements. The task would then be to retrieve the effective constitutive parameters (ϵ , μ) of a slab of the electromagnetic material from the measurement of S parameters. The retrieval process should ideally be independent of the slab thickness, yield continuous functions of parameters with respect to frequency, and satisfy the physical requirements for passive materials. Upon successful retrieval of the constitutive parameters, the frequency range where retrieval results can be used for propagation, scattering, and radiation problems need to be carefully identified.

In order to retrieve the effective permittivity and permeability of a slab of metamaterial or complex engineered medium, we can characterize it as an effective homogeneous slab. In this case, we can retrieve the permittivity and permeability from the reflection S_{11} and transmission S_{21} data calculated from the numerical simulations or obtained via measurements. For a plane

wave incident normally on a homogeneous slab of thickness d with the origin coinciding with the first face of the slab, S_{11} is equal to the reflection coefficient, and S_{21} is related to the transmission coefficient. The S parameters calculated from the numerical simulations can be used to retrieve the constitutive parameters. In particular,

$$Z = \pm \sqrt{\frac{(1 + S_{11}^2) - S_{21}^2}{(1 - S_{11}^2) - S_{21}^2}}$$

$$e^{ikd} = \frac{(1 - S_{11}^2 + S_{21}^2) \pm \sqrt{(1 - S_{11}^2 + S_{21}^2)^2 - 4S_{21}^2}}{2S_{21}}$$

where there are two sets of consistent solutions for (Z, e^{ikd}) . The permittivity and permeability can be found from the impedance and propagating factor. In the expression, k denotes the wavenumber of the wave in the medium and Z is the impedance of the medium. When this method is used to retrieve the effective parameters (index of refraction, impedance, permittivity, and permeability) of EM materials from transmission and reflection data, additional attention is required in the following: determination the effective boundary of the medium, and instabilities due to the noise contained in the scattering parameters where the retrieved parameters at some specific frequencies are not reliable. With the mixing formulas and the retrieval method, basic digitally designed EM materials can be effectively modeled, optimized, and characterized.

5. RAPID PROTOTYPING OF ELECTROMAGNETIC MEDIA DEVICES

Prototyping and laboratory/factory demonstration are integral parts of the product development, maturation and manufacturing process. The manufacturing industry has gone from prototypes made by skilled craftsmen that had long lead times to rapid prototyping that produces accurate parts from CAD models in a few hours using a completely automated process. There has been a significant interest both by government and private industry in application of such processes with the vision of reinvigorating manufacturing in the United States [56]. This interest has spurred the exponential growth in development of fabrication techniques with varied capabilities such as different materials (varying structural and mechanical properties) to resolution (providing a range of feature sizes) [24]. In the context of EM devices and media, these techniques can instead be applied to realize different devices that offer electrical and magnetic properties that can be altered from pure dielectrics with a wide range of refractive indices to conductive materials, all of which can be patterned and molded into geometric structures of macro-/micro-/nano- size features depending on the resolution of the fabrication method [31, 32, 57]. The same advantages of short turnaround time still apply in the research arena. Conventional research paradigms that use ‘material’ to ‘function’ flow can be slow where the specific natural material is studied and characterized [58]. Often, the optimal material for the application with respect to EM behavior is not discovered; design and rapid prototyping methods that change this research flow to ‘function’ to ‘material’ offer a great alternative to this process as shown in Figure 1 and Figure 2. The research of natural materials, however, still continues to contribute to the research field even in the case of rapid prototyping, where material science can enable new fabrication abilities (e.g. nanoparticle loaded polymers that can be ink-jet deposited enable unique plasmonic fields in a device) [59]. Prototyping processes can be classified into two classes: (i) Subtractive manufacturing: used in traditional fabrication and involves removal of material by methods such as drilling on a macroscale and lithography on a micro/nano scale; (ii) Additive manufacturing:

newer technology where a 3D object can be made based on a predefined digital model [24, 60]. Examples include 3D printing on a macro-scale [16, 57] and ink-jet deposition of nanoscale structures [31, 56].

In this review paper, we will focus on additive manufacturing processes and their application to the field of EM structures and engineered media. AM encompasses a variety of techniques that can be used to build structures from a digital model and is often referred to as 3D printing. Most AM techniques are layer-by-layer processes in which thin layers of materials are deposited according to an input digital file. The National Additive Manufacturing Innovation Institute (NAMII) lists the following as benefits of AM: shorter lead times, mass customization, reduced parts count, more complex shapes, parts on demand, less material waste, and lower life-cycle energy use [56]. For defense applications, the tailoring to specific applications as well as ability to manufacture with little investment in infrastructure directly translates to reduced cost. There are several additive manufacturing processes, proprietary machines and methods that are currently in use. Most of these methods can be broadly classified into categories that share processing similarities. The ASTM International defines seven categories in the Standard Terminology for Additive Manufacturing Technologies [61] as following: (i) Binder jetting: liquid bonding agent is selectively deposited to join powder materials [62]; (ii) Directed energy deposition: focused thermal energy (e.g., laser, electron beam, or plasma arc) is used to fuse materials by melting as they are being deposited [63]; (iii) Material extrusion: material is selectively dispensed through a nozzle or orifice [64]; (iv) Material jetting: droplets of build material (e.g. photopolymer and wax) are selectively deposited [65]; (v) Powder bed fusion: thermal energy selectively fuses regions of a powder bed; (vi) Sheet lamination: sheets of material are bonded to form an object [66]; and (vii) Photopolymerization: liquid photopolymer in a vat is selectively cured by light-activated polymerization [61]. Most of the applications discussed below use material jetting, material extrusion or directed energy deposition processes, but any of the other categories of fabrication methods can be adapted to achieve the same structures. The methods serve as a means to produce the unique EM behavior in a quick prototyping environment while providing the precision needed for the structures. As long as the resolution and available intrinsic material properties fit the applications, we believe that any of the processes can be easily adapted to the structures discussed below.

5.1 Macroscaled features

We begin the discussion with structures that use micron-sized or larger features which can be used as engineered materials in the RF/microwave and longer wavelength regimes and for devices within the geometric limit at optical frequencies. This stems from the fact that a micron-size cell still has subwavelength dimensions at RF frequencies and thus an array of constituent unit cells can be modeled as a bulk medium with cumulatively representative EM properties that affect the waves impinging on it or passing through it. In the optical regime however, the size of such structures would be large compared to the wavelength of light and thus they behave like devices rather than materials. Both regimes are discussed with representative examples of materials and devices.

In the microwave regime, fabrication of EM structure and devices is traditionally carried out using patterned dielectric substrates that may be partially or fully coated with a conductive material. Many of the engineered media applications in this regime, have been demonstrated using a stacked approach where unit cells such as the double fishnet structures are periodically

arranged to form an array and then stacked with precise registration to act as a 3D material. In the more complex metallized designs in both 2D and 3D media, we see the use of printed circuit boards emerge as the prototyping solution of choice, combining material removal through machining and etching with material addition by soldering and plating. Some examples of 3D media are shown in Figure 4. A large number of existing 3D designs have been assembled from multiple PCB layers to increase dimensionality [67]. While attempts have been made to make advances to 3D structures using planar techniques in combination with through vias and stacking with alignment, the processes described are still planar methods and have their inherent drawbacks.

For example, strongly chiral media [68, 69] for circular dichroism or large anisotropy [70] is difficult to achieve using layered structures. Some publications have researched the use of multilayer stacking approach [71] where a structure is fabricated using lithography, planarized and then subsequent layers fabricated using interlayer lateral alignment but practically the number of layers that can be successfully stacked has been restricted [56, 72]. Truly bulk 3D media have been also demonstrated with such stacking techniques although they are restricted to certain propagation directions and/or polarization [73]. Most of the currently demonstrated designs are very thin materials which in the wavelength of operation act like a monolayer of atoms and suffer from high losses which make them unviable options in practical devices [33]. The biggest challenge lies in implementing such structures as large-scale materials that are thick, or 3D with low losses.

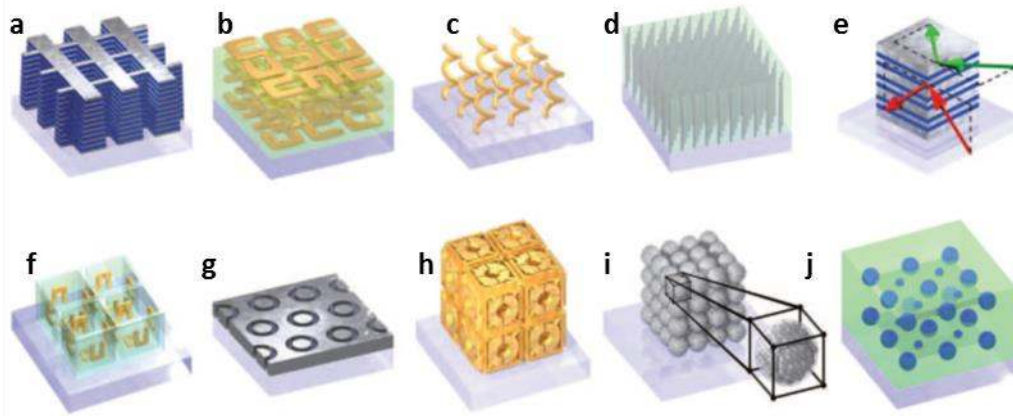


Figure 4: Examples of 3D metamaterial structures (a) Double-fishnet metamaterials, (b) Chiral metamaterials via stacked electron-beam lithography, (c) chiral metamaterials made via direct-laser writing and electroplating, (d) hyperbolic metamaterial, (e) metal-dielectric layered metamaterial composed of coupled plasmonic waveguides, (f) 3D split-ring resonators, (g) wide-angle visible negative-index metamaterial, (h) Connected cubic-symmetry negative-index metamaterial structure, (i) Metal cluster-of-clusters visible-frequency magnetic metamaterial, and (j) All-dielectric negative-index metamaterial composed of two sets of high-refractive index dielectric spheres arranged on a simple-cubic lattice [74]

Additive manufacturing techniques may be used to fabricate such structures and also fulfill the requirement of reduced losses by enabling the construction of more complicated 3D designs that can be either purely dielectric or metal-dielectric. The 3D materials and devices that will be presented in this section primarily used extrusion deposition, material jetting, and powder bed fusion during fabrication. Two sets of materials are usually employed; one for the part material and one for the support material which provides stability during the build but breaks away easily without surface damage after the part is complete. The common polymers used for part synthesis range from optically transparent to opaque materials in a variety of colors with varying mechanical properties that provide the user flexible rubber-like as well as rigid materials depending on the application. The support material is usually a softer substance that can either be removed using a wet chemical etch or water pressure. The following provides a brief description of some of the commonly used processes. Extrusion deposition is also known as fused deposition modeling where a movable head deposits a thread of molten material for a 2D pattern through an extrusion nozzle which is turned on/off by a computer-aided manufacturing software package to print the design defined by a CAD file [24]. Metals or polymers can be shaped using this process. Another set of fabrication methods employs material jetting. This class of processes is very similar to ink-jetting in two dimensions; part and support material is jetted through nozzles to build a 3D object that is defined in a software file. Most of these systems support a wide range of polymers, and geometrically complex structures are enabled by the use of both build and support material. The build material can be a photopolymerizing resin that is cured using ultraviolet light in conjunction with a CAD model. The gaps in the cured polymer are filled with the support material which is a wax or gel-like substance that is added after every raster scan during the build. This material is washed off after the build and allows the user to build challenging structures such as overhangs or protrusions. Another AM fabrication technique that is used to fabricate EM structures is selective laser sintering, where granules of base material are fused together to make a part in a layer-by-layer fashion adding granules that are fused as the part is built up. The unfused material acts as a support to fragile structures during the build. Polymers, ceramics and metals can all be patterned using this process [24].

Finally, we present some pertinent examples that illustrate the applicability of AM processes described above to the design and fabrication of complex EM materials and devices. We begin with materials and devices for application in the RF regime that have been fabricated using AM processes. All dielectric complex media offer potential to overcome prohibitive losses that are presented by metallic resonators used in RF EM media and metamaterials. However, as mentioned before, they interact weakly with waves and hence require more complex geometries such that their dispersion and anisotropy is well engineered. One example of such media was presented where the EM media was designed using plane wave engineering method and square and hexagonal arrays optimized to be uniaxial in three dimensions (Figure 5). The samples were fabricated with polycarbonate using fused deposition molding, and the measured material property tensors agreed well with the theoretical models [8].

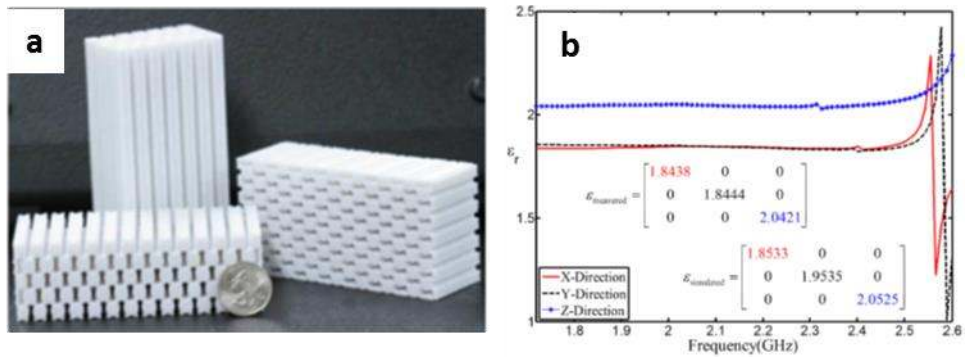


Figure 5: (a) Manufactured anisotropic metamaterial, (b) Measured dielectric tensor of material in (a) [8]

The next category in the context of RF devices is printed 3D components. Antennas have remained the center of research as capacity needs increase with multimedia data and size constraints are tightened [75], especially in applications such as satellites [76] and mobile devices where size and weight are critical [77]. 3D antennas provide design flexibility needed in such systems by allowing the designer the ability to work in a volumetric space, not just 2D planar area using non body-of-revolution and asymmetric configurations [78]. This gives the designers more control over antenna parameters such as radiation patterns, gain, polarization and aperture efficiency as well as the flexibility to explore alternative antenna geometries [79] that meet some given mechanical performance while maintaining EM performance [80, 81]. One such antenna that was recently demonstrated was an electrically small spherical wire antenna with a radiation quality factor close to the physical lower bound [73]. The antenna was fabricated in plastic using 3D printing and then metalized using conductive paint in a post-processing step. Such a design would be very difficult to fabricate in any other way. Other tools for manipulation of radiation are microwave lenses and reflectors which can be used to modify phase of a wavefront as desired [26, 82]. They can be used to perform such functions as obtaining asymmetrically flared beams using line sources, or combinations of the two elements can be used to produce pencil beams.

In this regime, lens design and fabrication requirements are far more forgiving than in the optical domain where surface imperfections can lead to severe aberrations. This allows the use of soft thermoplastics such as polystyrene instead of glass which lends itself perfectly to AM fabrication techniques. Microwave lenses can also be made from metal plates such as those used for phase correction in sectoral horns. Therefore, lenses at RF wavelengths can be fabricated using homogenous or spatially inhomogeneous dielectric material, where traditional optics dictate the geometry of the lens, or selective/full metallization. In a recent publication, our research group demonstrated a 3D graded index lens designed to operate at X-band and fabricated using a polyjet rapid prototyping method to fabricate to implement the effective medium [82]. The GRIN lens (Figure 6 (a) and (b)) with radially varying refractive index gradient showed a focus of ~18cm as designed and was built with isotropic, inhomogeneous dielectric material using mixing ratio of air/voids and a polymer which dramatically improves size and weight of currently focusing lenses with homogenous refractive index that are curved. The unit cell geometry chosen for this lens was a square dielectric with a varying center void volume of 0-97.3 mm³ defined by the extremes with no hole at one extreme (solid dielectric block unit cell) and the other extreme with the largest hole dimension dictated by the minimum thickness that can be fabricated

depending on the strength of the chosen dielectric material and the printer resolution (hollow unit cell with thin walls) [29].

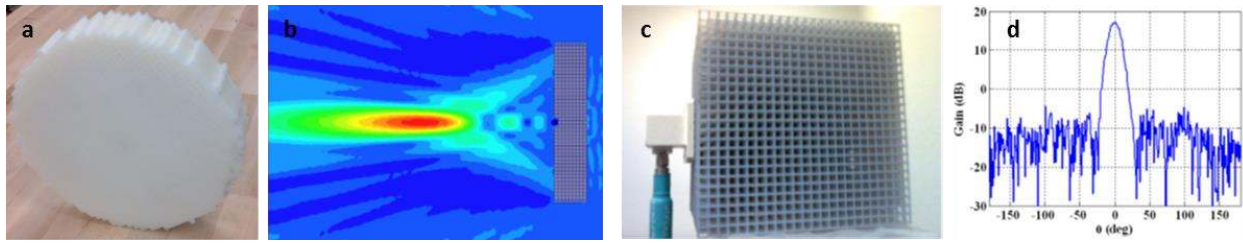


Figure 6: Examples of lenses fabricated with AM (a) GRIN lens fabricated using 3D printer. The fill factor decreases radially outwards and the voids are visible in the unit cells as you approach the periphery of the lens, (b) Results of 3D electromagnetic simulation of a homogenized 3D lens (with actual unit cells) carried out in HFSS: electric field shows focus at location of 25 cm, [29] (c) Experimental setup, the Luneberg lens is fed by an X-band waveguide mounted to the surface of the Luneberg lens, (d) Measured radiation pattern of the Luneberg lens at 10 GHz [83]

Min *et al* also used a polymer jetting rapid prototyping process to fabricate a 12 cm diameter 3D Luneberg Lens designed for the X-band based on the mixing ratio of air voids and a polymer (Figure 6 (c) and (d)). The lens had individual unit cells that measured 5 mm^3 where polymer was surrounded by air voids. The half-power beam width and gain of the lens were 14° and 18 dB respectively, and no obvious side lobe is found above the noise floor. This design showed significant cost advantages with a more convenient and faster fabrication process compared to traditional Luneberg lens. Another lens that has been demonstrated using rapid prototyping is a plano-concave lens built from a 3D self-supporting metamaterial structure with a negative refractive index between 10 and 12 GHz, low loss, recognizable focus and free space gains above 13 dB. The lens that was metallized using post-processing after 3D printing had dimensions were $255 \times 225 \times 40 \text{ mm}^3$ with a frequency dependent focal length of 6–10 cm [83]. These examples show the efficacy of using AM processes to fabricated RF components with micro- and macro- scale features with lower weight, size and cost while improving/maintaining EM performance.

While the previous section focused on microwave components where some of the individual features had subwavelength dimensions for that frequency range, this section focuses on devices designed for the optical frequency bands with macroscale dimensions and can thus be described using the Eikonal approximation or ray optics. 3D printing methods are being used to design and manufacture solutions for light propagation, focusing and manipulation. In these applications, sensitivity of the optic to imperfections can lead to wavefront distortion and aberrations. Advances in AM processes can produce high quality structures that do not require post processing steps such as polishing, grinding and coloring to produce optically smooth and full color devices. A recent demonstration of optical grade lenses used UV-cured polymer jetting to create optical components for light emitting diodes (Figure 7 (a-d)) [57]. A high resolution piezoelectric print head is used to deposit discrete drops with interspersed delays which allows

for better surface wetting and diffused surface tension delivering complex, optical quality surfaces without post processing steps such as polishing. Since each shape or lens that can be fabricated using the high resolution print technology used by LuxExcel consists of several tiny droplets, symmetrical as well as “freeform” structures (Figure 7 (e) and (f)) can be made that would be very difficult and expensive to fabricate otherwise [84].

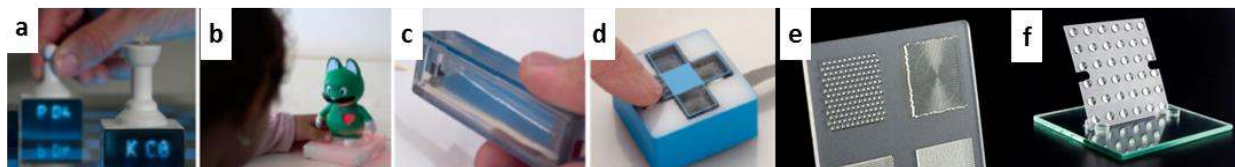


Figure 7: Custom optical elements fabricated with 3D printing. Such elements embedded in interactive devices, opening up new possibilities for interaction including: unique display surfaces made from 3D printed light pipes (a) Novel internal illumination techniques, (b) custom optical sensors, (c) embedded optoelectronics, (d) Mechanical structure of an interactive device (similar to (c) [57], (e) 3D printed lenslets and printed optics, (f) Customized 3D printed lens array [84]

In addition to lenses, mirrors, prisms and beamsplitters can be emulated using clever design that utilizes air voids to guide and manipulate similar to the structures presented in the RF components section. Other interesting structures can be made by combining materials with different refractive indices to guide light using total internal reflection or blocking transmittance of light in sections using opacity at certain wavelengths to minimize crosstalk and noise due to energy leakage. An example from the first category where an air volume is encompassed by a polymer is a light pipe which is commonly used to guide light from point to point similar to an optical fiber but for much smaller distances. Typical applications are displays, sensors and optical platforms where light pipes are combined with optoelectronics and lenses to shape an emitted beam and control its directionality [57]. AM processes allow arbitrary geometries to be created in a single print job without mechanical assembly, chemical bonding or fusing with heat, all of which add a manufacturing step and may compromise strength of the part.

5.2 Nanoscaled Features

Next we move the discussion to nanoscaled features which are primarily useful in application from the THz to optical frequency regimes. The applications of such devices and media include photonics, high speed information processing and storage, microbiology, surveillance, energy harvesting, defense technology as well as sensing platforms to name a few [85, 86]. The structure of materials and the intrinsic properties that describe the cumulative behavior of media in the EM domain centers on basic wave-matter interactions. As fabrication techniques continue to advance and enable submicron scale structures, the prospect of tailor-made materials properties become a reality at the appropriate operational wavelengths by exploiting geometrical elements and defined symmetries. Traditionally used methods to fabricate these devices are based on layer by layer deposition in conjunction with lithographic techniques, such as electron beam lithography, to define the features [87]. These methods have been very successful in creating 2D patterns on the micron and nanometer scale and have allowed the extension of Moore’s law and leaps in

computational power. The fabrication of 3D structures using these methods requires cumbersome and sometimes inaccurate registration schemes for stacking which makes it challenging to fabricate practical devices and also difficult to make truly 3D structures with anisotropic properties like chiral media [88].

3D fabrication techniques are being developed to address this technology gap. These methods can be classified into self-assembly [89] or construction based techniques. Self-assembly techniques utilize thermodynamic forces to place components and build features into requisite structures over large areas in a cost and time effective manner[90]. Structures manufactured using these methods are fraught with errors that result from fabrication defects and are limited by the achievable accuracy dictated by weak van der Waal type forces that are difficult to control with high spatial precision [91]. In this paper, we will focus on construction based methods which fall under the category of additive manufacturing. One of the advantages of using these techniques versus traditional methods is the ability to fabricate arbitrary 3D geometries at the nanoscale which allows them to be further applied to build functional micromachines in addition to photonic components.

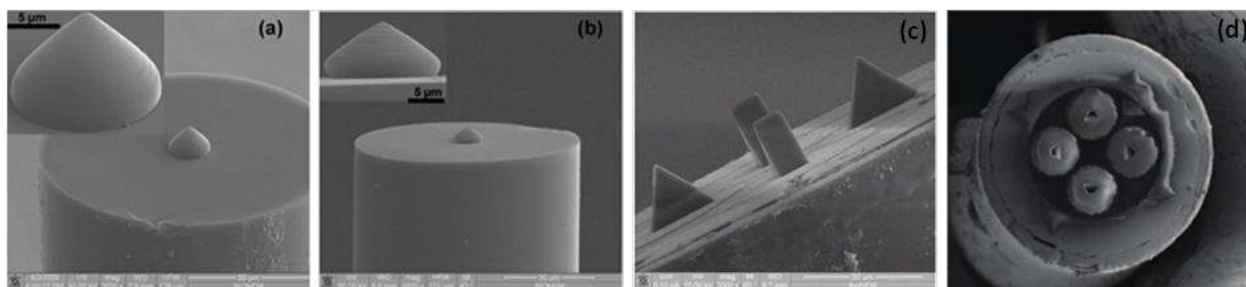


Figure 8: Microscale lenses fabricated with two-photon lithography (a) SEM image of a fabricated conical lens with 80° apex (enlarged view in the inset), (b) SEM image of a fabricated conical lens with 120° apex angle (lateral view in the inset) [92] (c) SEM image of optical tweezers end facet, [93] (d) SEM image of miniaturized optical tweezers [94]

We will focus on 3D jet printing, two or multi photon lithography, and focused electron beam induced deposition, which have been explored to fabricate devices and media with feature sizes that beat the diffraction limit and can provide spatial resolution on the order of a few nanometers (Figure 8) [95]. This section gives a brief overview of the processes that we will focus on. Inkjet [96] and electrohydrodynamic jet (e-jet) printing uses thermal, acoustic or electric field energy to pump pressure controlled inks onto a substrate through a capillary or nozzle [65]. The fine fluid flow enables nanometer sized feature deposition at a relatively fast pace. The next technique, focused electron beam induced deposition (EBID), is a direct-write lithographic process where features are defined by scanning a gas-phase focused electron beam on a substrate. No significant pre-or post-processing is required for this method, and since most of the instruments employ electron microscopes, in-situ characterization of the sample is possible [97]. The resolution provided is defined by the spot size or diameter of the focused beam which has been varied from micrometers down to sub-Angstrom sizes [59, 98]. The next method that is often used in 3D nanoscaled patterning is two or multi photon lithography [92, 93]. This method was developed to overcome the depth resolution constraints of single-photon stereolithography [94, 98]. A photopolymer is radiated with near infrared light. Two photons are simultaneously

strongly absorbed in a single event at the focal point in the photopolymer with a quadratic intensity dependence which produces solidification and definition of features far smaller than the diffraction limit. Arrays of 3D structures can be fabricated by scanning either the laser focus or the sample. Some examples are shown in Figure 9.

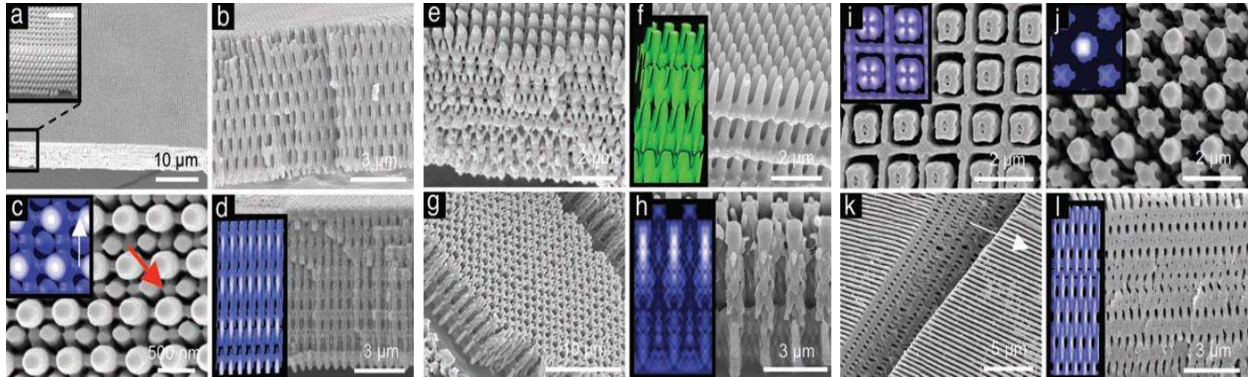


Figure 9: SEM of 3D nanostructures: Insets present the corresponding computed optical intensity distributions. (a) 3D nanostructure patterned with mask 1 over a large area, limited only by the size of the mask, (b) (110) cross-sectional view of the structure in (a), (c) Top view of the same structure (red arrow points to an ~ 100 -nm structure in width). Inset shows modeling (arrow indicates the direction of polarization of the exposure light). (d) (100) cross-sectional view of a 3D nanostructure formed with mask 1 and the filtered output of the 365-nm emission line from a conventional mercury lamp. The modeling (inset), which assumes perfect coherence, accounts accurately for the shape of this structure. (e) Structure generated with mask 2 and 355-nm light, (f) Structure generated from mask 2 with 514-nm laser light. The top layer of this structure, which is shown in the modeling, peeled off because of its thin connecting features to the underlying structure, (g) Structure generated with mask 3, (h) Close-up view of tilted (100) facet of this structure. The modeling in the inset corresponds to a cross-section cut through the middle of the pillars, (i) Magnified view of top surface of this structure; inset shows modeling results. (j) Bottom surface, inset shows modeling results. (k) Stack of sealed nano-channels made by using mask 4. The polarization direction is parallel to line (arrow), (l) Magnified cross-sectional view, inset shows modeling results [99]

There are several applications where these processes have been used. In the following sections, we present some examples that demonstrate their efficacy in the photonic regime. We begin our discussion with 3D photonic crystals [100, 101] which have garnered much attention in recent years due to their potential application to develop thresholdless semiconductor lasers, single-mode light-emitting diodes, ultra-compact low loss waveguides for high speed information processing, etc. [102, 103] The biggest challenge in the development of these devices is the precise fabrication required to build them which demands precise structural control in three dimensions [104-106]. Two-photon lithography has been used to develop masks with conformable elements [99] and molded reliefs that allow for nanopatterning by close contact exposures using near fields [107, 108]. These masks were recently used to fabricate Si/air

photonic crystals over large areas with high fidelity to the design geometries consistent thus displaying properties that agreed well with theoretical results [102].

Further research on photonic crystals has explored ways to control and confine light in small dimensions using functional defects that trap/emit light in precise locations which is very desirable in optical computing and integrated optical processing [109]. Complex defect structures can enable the control of light propagation through localization around the defect which can also dramatically reduce emission lifetime [110]. Two-photon lithography [111] has also been used to direct write defect structures in holographically fabricated 3D photonic crystals (Figure 10). The combination of two optical lithographical techniques viz. holographic lithography, which can provide coverage over large areas, and two-photon lithography, which can fabricate defects of high resolution spatial placement and shape, leverages the advantages of both methods to fabricate nanoscaled features over very large areas in a relatively short time period [110]. One illustrative example shows light-trapping at 632nm based on a 2D hexagonal lattice with a missing central pillar resulting in a micro-cavity on the surface of a SiO₂ prism. This structure creates a finely focused low volume light point source when excited by total internal reflection illumination and could be potentially applied to single molecule detection using a measurement technique like fluorescence correlation spectroscopy [109]. Previously published work has demonstrated the use of two-photon lithography to create defects in photonic crystal templates, such as a large area woodpile in SU-8 as well as dipentaerythritol penta/hexaacrylate (DPHPA) with photoinitiator. In addition to multiphoton lithography, focused EBID has also been effectively used to create 3D photonic crystals with predefined defects for extreme light localization [110].

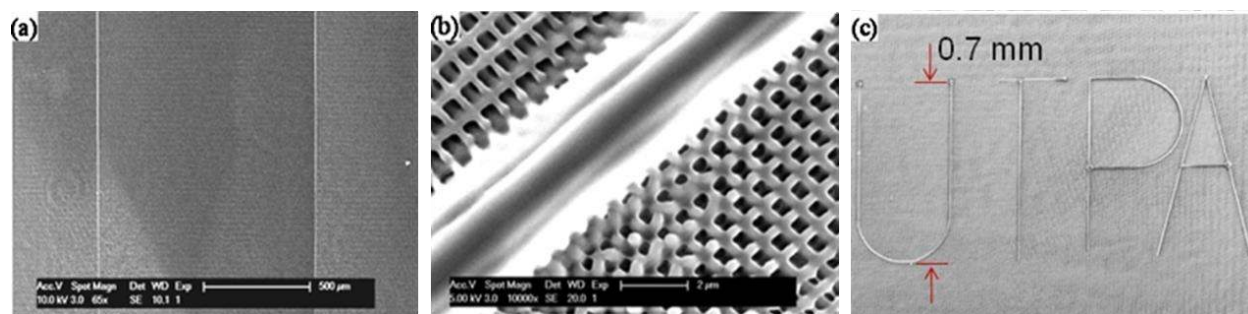


Figure 10: 3D printed photonic crystals with defect lines (a) Large area SEM image of defect lines fabricated in holographic photonic crystal (PhC) template; (b) Enlarged view of SEM image of defect line in 3D PhC template; (c) Defect structures in UTPA letters are fabricated in 3D PhC template. The height of letters is 0.7 mm as designed in the motion stage control program [110]

Nanoscaled additive manufacturing processes have also been used for nanoscale object manipulation, mask repair and fabrication of periodic arrays. Recently, a modified version of EBID called liquid phase EBID was used to deposit silver nanoparticle arrays with high purity by utilizing precursors without carbon/phosphorus based architectures which mitigate undesirable impurities of organic and inorganic ligands (Figure 11). The geometry of the nanoparticles can be changed by modifying the dose or beam astigmatism to tune the localized

surface plasmon resonance. The particles demonstrated had diameters ranging from 55-100nm which gave rise to resonance wavelengths from 550-600nm [59]. Nanodot and nanopillars have also been fabricated into linear arrays for plasmonic waveguides using EBID where the metal nanostructures were deposited directly by using an electron beam (ionization energy $\sim 5\text{-}50\text{ eV}$) to dissociate metal from an Au precursor gas (Dimethyl Au (III) Fluoro Actylacetate) in a predefined reaction region on the substrate. The metallic nanopillars had sizes of 40-70 nm and were spaced 15-30 nm apart to develop polarization sensitive plasmonic waveguides. Such nanopillars have also been fabricated using electrohydrodynamic ink-jet printing which allows for very high resolution nanoscopic placement. The third dimension is controlled by autofocusing by local electrostatic field enhancement which enables very high aspect ratios. Features sized down to 50nm have been obtained with aspect ratios of 4 in the third dimension [112]. The polarization sensitivity is measured by recording the transverse and longitudinal resonance spectra at 528 nm and 660 nm which agree with the theoretical predictions of 525 nm and 700 nm [113].

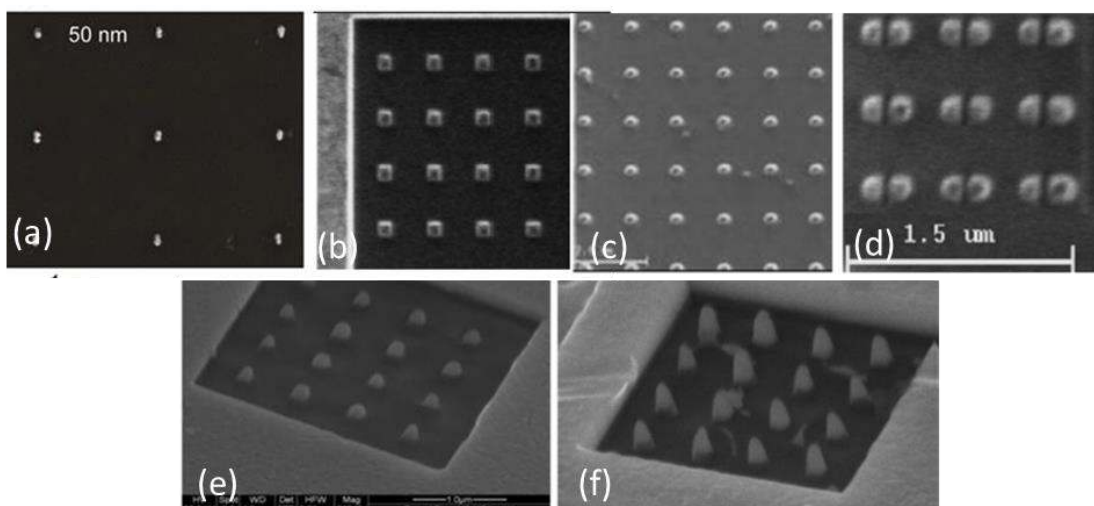


Figure 11: Nanoparticle arrays fabricated using electron beam induced deposition (EBID) (a) SEM images of rod shaped Ag deposits created with a stigmated electron beam at dose of 50 pC [59], (b) A 4 x 4 square nanopillar array, developed by FIB, at the tip of a 50 nm gold coated multimode optical fiber. Each square has an edge dimension of 200 nm, (c) Nanopillars with an elliptical cross-section (d) Dimer nanopillars separated by $\sim 18\text{ nm}$ (e) Au nanopillars formed by FIB. SEM was taken at a 30 degree tilt (f) Pointed gold nanorods formed by employing FIB milling [112]

In addition to metallic arrays, EBID has been successfully used to grow nearly pure, magnetic, cobalt nanostructures (diameter $\sim 30\text{ nm}$) with possible applications to nano-Hall probes using arrays $\sim 100 \times 100\text{ nm}^2$ and sensitivity in the range of $0.1\ \Omega/\text{T}$. Magnetic nanowires have recently been suggested as candidates for 3D memory devices. 3D magnetic nanowires ($\text{Co}_2(\text{CO})_8$) with very large aspect ratios (~ 100) can be grown using EBID by combining the micromanipulation, Kerr magnetometry and magnetic force microscopy. This research group also demonstrated that individual nanowires can be magnetically switched using direct probing by magneto-optical Kerr effect. The nanowires demonstrated (Figure 12) showed high purity,

low roughness and functional magnetic properties. Two loop nanospirals and plasmonic nanoantennas have also been demonstrated using EBID [114].

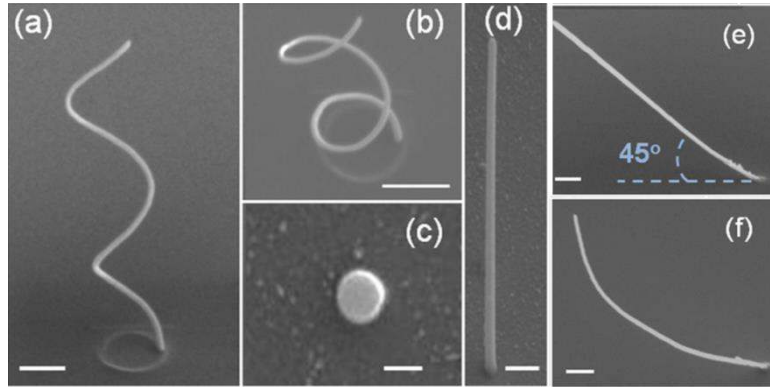


Figure 12: (a) and (b) Different views of a double loop nano-spiral, (c) Top view of a straight nanowire, (d) and (e) Lateral view of nanowires grown at 0° and 45° respectively, to the substrate plane, (f) Curved nanowire after magneto-optical Kerr effect measurements, The scale bar is 500 nm in all images, except in (c), where it is 100 nm [114]

Other photonic components, complex optical media and metamaterials [7] have also been designed and demonstrated using additive manufacturing techniques. One interesting demonstration was that of 3D single wall carbon nanotube/polymer composites using two-photon lithography. In this study, a femtosecond near infrared laser beam focus spot was scanned to fabricate arbitrary shaped 3D nanostructures and nanowires with lateral dimensions as small as 200nm with good mechanical and electrical properties (Figure 13) that would lend themselves to applications not only in photonics but also in 3D MEMS and NEMS [115].

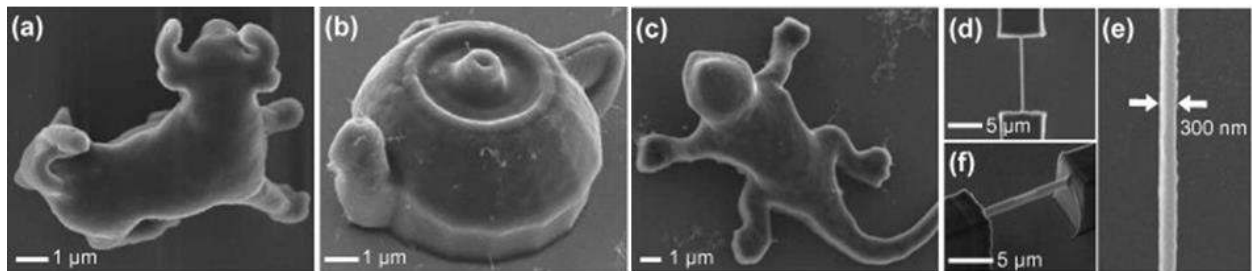


Figure 13: 3D micro/nano structural SWCNT/polymer composites are fabricated by using two photon lithography. The structures shown are a (a) 8 μm long microbull, (b) micro teapot, (c) micro lizard, (d) nanowire suspended between two microboxes, (e) magnified image of (d) and (f) perspective view of the nanowire [115]

Metamaterials have recently been demonstrated in the optical regime [116, 117] with reasonably low losses, but building 3D bulk metamaterials on a manufacturing scale remains a challenge using conventional fabrication processes and stacking. One avenue to making these materials a viable option in practical applications is additive manufacturing processes [118, 119]. Rill *et al* have used 3D two photon lithography and silver shadow evaporation to fabricate a bianisotropic negative index metamaterial (Figure 14 (a)) that shows a negative real part of the refractive index

at $\lambda=3.85\mu\text{m}$ [120]. Other than classic negative index media, 3D metamaterials have also been used to design perfect absorbers/reflectors where a microstructured surface can be switched between a perfect absorbing and reflecting state simply by changing the polarization of incident light. The structures that were used in these prototypes consisted of 3D U-shaped resonators (Figure 14 (b)) using two-photon lithography which are expected to dissipate the heat produced in the absorbing phase easily [121].

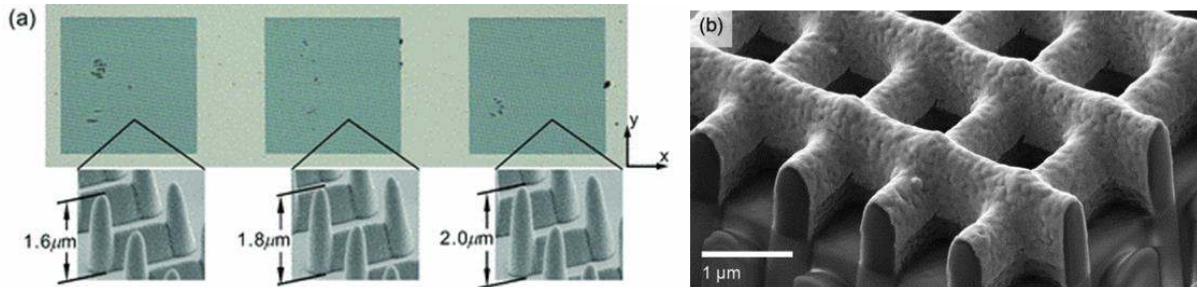


Figure 14: (a) Optical micrograph of standing U-shaped resonator (SUSR) arrays with different heights. The insets show FE-SEM micrographs of the SUSR unit in each array respectively [120]. (b) Oblique-view electron micrograph of a metamaterial structure fabricated by direct laser writing and silver shadow evaporation that has been cut by a FIB to reveal its interior [121].

Apart from photonic bandgap structures, many devices have been produced with nanoscale precision using additive manufacturing processes. Atwater *et al* used two-photon lithography to direct write microphotonic parabolic light directors (Figure 15) that exhibited strong beam directivity with a beam divergence of 5.6 that agreed well with theoretical prediction based on Eikonal limit and full-wave EM simulations. The biggest advantage of using this technique was the ability to expose a well-defined 3D voxel on the nanoscale in a precise location determined by the waist of the laser beam. While compound parabolic concentrators have been demonstrated at the macroscale, this demonstration showed the efficacy of the fabrication method as well as the device at a microscale using arrays of concentrators built on top of solid-state photonic devices. The collimation properties of these structures could be used in controlling emission from light-emitting diodes or even to improve the collection efficiency of solar cells/detectors [104].

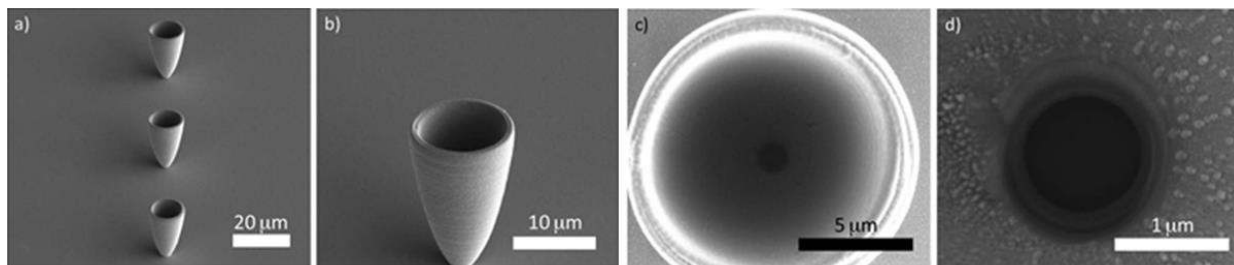


Figure 15: (a) SEM image of array of parabolic reflectors coated with silver; (b) SEM image of single paraboloid; (c) plan view of single paraboloid with light transmission aperture visible at bottom center; and (d) close-up of light aperture etched with a focused ion beam [104]

Both complex media and devices discussed above exploited the advantages of additive manufacturing processes to directly build their constituent structures. There are indirect routes that additive manufacturing can be used to pattern and fabricate structures. For example, recently a research group headed by S. Maruo used two-photon lithography to fabricate a 3D PDMS template that can be used to replicate complicated 3D microstructures such as movable microgears and microtweezers. Other than provide an alternate route to building soft-molds, this process also helps expand the range of materials that can be accessed for patterning beyond photopolymers and photoresists, while maintaining the resolution advantage of two-photon lithography. To this end, the group used slurries of ceramic nanoparticles and beta-tricalcium phosphate microparticles which were dried and sintered to fabricate a 3D ceramic microstructure. Ceramics find applications in many systems where high mechanical strength, heat resistance and biocompatibility are desired. Other combinations of polymer and nanoparticles such as silica can be used to form optically transparent 3D microchannels that can be used in microelectromechanical systems and photonics [122-124].

5.3 Conformal Structures

3D devices and media do not have to be relegated to the strict definition of freestanding or stacked structures. Similar interesting properties can be obtained from materials or devices that can conform to various 3D shapes, and in this paper we consider such structures as a class of 3D media. A conformal structure is by definition a device or structure that conforms to a surface shaped by considerations other than EM such as aerodynamic performance [125]. The purpose of building conformal structures is to integrate them with the support so as not to change the mechanical/structural properties [126]. For example integrating antennas into aircraft skin can reduce drag of an otherwise mounted device and thus minimize fuel consumption [127]. The need for conformal antenna arrays with radiating elements on the surface of a cylinder, sphere, cone or a similar smoothly curved surface is important in large-sized apertures like satellites and airborne radar systems where size, weight and EM performance all need to be carefully balanced [128]. Other applications that can benefit from conformal devices include filters and other coating-like structures in optical imaging where the field of view can be maximized with a spherical shape [129].

The first example of conformal structures that will be discussed is conformal antennas and arrays. Complex antenna arrays with non-planar geometries have been implemented in the past using multiple layers or tiling schemes which may involve intricate and time-consuming assembly steps [130]. Some designs based on canonical geometries have utilized directive deposition through shadow masks [131] or flexible contact masks [132] to mitigate defects such as folding, stretching and cracking that can result from a post-processing step [133]. Masks, however, have been implemented successfully only in single curved surfaces such as cylinders with an added restriction of patterning smooth elements. Direct writing processes, in contrast with robotic styluses can trace curved patterns on complex surfaces. In these processes, metallic ink is deposited in thin layers and therefore is time-consuming and restricted by the conductive inks available [134-136]. Recently, a 3D conformal shadow mask was used for selective metallization of antenna patch elements and feeds to form a 2x2 array on a doubly curved surface (Figure 16(a)) with fully conformal metallic ground plane that operated at 4GHz [137, 138].



Figure 16: (a) Conformal antenna patterned by sputtering [138], (b) Small spherical wire antenna covered with conductive paint [73], (c) Optical image of an antenna during the printing process [135]

A further step in a fully conformal design was demonstrated by the Lewis group, where conformality not only helped adapt the antenna to a given shape but also helped to achieve 3D electrically small antennas (Figure 16 (b-c)) that approached the fundamental limit for size significantly better than rudimentary monopole designs [135, 139, 140]. The antennas were fabricated by conformal printing conductive inks onto convex and concave hemispherical surfaces in meander lines. Since this approach used direct printing, it can be rapidly adapted to different designs, surfaces, applications and operating frequencies with the simple alteration of a design file. This improves speed of design and adaptability relative to the mask technique where a new set of masks is required for each design change. The particular design that was demonstrated was based on the principle that antennas/sources placed in spherical volume closely approach Chu's limit, yielding bandwidth improvements compared to their linear and planar counterparts. In this technique, the substrate is aligned and each antenna is printed on the curved surface using metallic ink deposited through a micro-nozzle using a design file. After printing, the antennas were heat treated to form highly conductive metallic traces [135, 136].

Antenna arrays are often coupled with lenses or filters that help to hone their response to the desired frequency or radiation pattern needed for the application. Frequency selective surfaces (FSS) or dichroics are used as filters, usually in frequency although sometimes they are applied to the angular spectrum. Conformal frequency selective surfaces are commonly constructed of periodic arrays of conductor segment or inverse surfaces with slots in conducting sheets and their resonant interaction results in transmission that is dependent on frequency and orientation of the incident EM wave with respect to the periodic structures. In the past, FSS prototypes have been fabricated using planar manufacturing methods. Recently, a conformal FSS in the shape of a paraboloid patterned with an array of cross-loop features was demonstrated using AM processes and using electron beam deposition for a stop band at 12.5 GHz with a 30dB drop in power transmission. The mask used to deposit the FSS features was fabricated using rapid prototyping technique and could easily be extended to other complex surfaces and structures by printing similar shadow masks using CAD designs and 3D printing [137].

Additionally, resonant structures have been demonstrated on simpler canonical surfaces with micromachining, electrodeposition and soft lithography pattern transfers [141]. Another example of a frequency dependent structure that was reported was a microwave X-band cloak. This device was only about one wavelength thick and was fabricated using a stereolithographic

polymer-based fabrication method. In the designed band, the shell eliminated the shadow and significantly reduced scattering from a large cylinder for incident plane waves in free space without the use of an immersion liquid or conducting ground plane [33]. It should be noted that fabrication of passive structures such as those used in FSS, filters, beam steering arrays, cloaks, etc. are comparatively simpler to design and fabricate than antennas, since there are no feed network considerations and the individual elements may or may not be connected for routing energy.

Similar research into printing components and media in the optical regime has also yielded interesting results. While there are several methods to accomplish conformality, we focus here primarily on nanomembranes (NM) since they lend themselves to various direct write methods discussed above, can include a range of inorganic materials and conjugated carbon compounds like graphene, and have been proved to be a very effective way to build both media and devices [142, 143]. We begin the discussion with EM media and then move to devices. Optical metamaterials have been fabricated to operate in the terahertz using electrohydrodynamic jet printing on flexible substrates thus lending themselves to successful application in conformal applications (Figure 17). The metamaterial demonstrated by this process was based on I-shaped $10\mu\text{m}$ width, silver unit cells with $5\mu\text{m}$ gaps and lengths of $110\mu\text{m}$ fabricated on a $5\times 5\text{ mm}$ polyimide substrate. This material exhibited a high refractive index measured using terahertz time-domain spectroscopy with a peak value of 22.19 at $\sim 0.5\text{THz}$ [119].

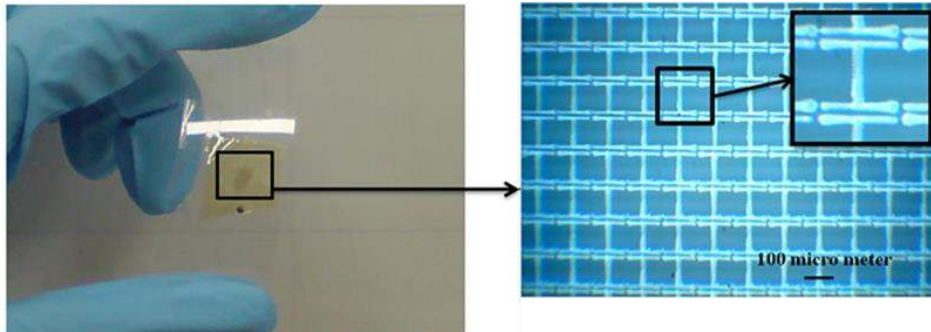


Figure 17: Photograph of printed flexible metamaterial designed to operate in the THz range [119]

Other than media, nanomembranes have also been used to fabricate flexible optoelectronic components such as photodetectors and lasers [144]. This is critically important in the advancement of flexible electronics and integrated circuits. Multiwavelength flexible photodetectors fabricated on a plastic substrate using single-crystal germanium (Ge) membranes. Visible photodetectors were grown using ion implantation by selectively doping Ge-on-insulator substrate and were dry-printed in a lateral p-i-n configuration followed by an annealing step. The photodetectors exhibited a quantum efficiency of 5% at 411nm and 42% at 633nm with -1V bias. The low quantum efficiency is presumed to be due to shallow penetration depth and high photocarrier recombination at surface traps which may be mitigated using surface passivation [145]. In addition to detectors, sources such as silicon hybrid lasers have also been demonstrated using NM technology by combining Si with III-V gain media. Yang *et al* demonstrated III-V

InGaAsP quantum-well heterostructure vertical cavity surface-emitting laser single-layer silicon sandwiched between photonic-crystal Fano-resonant Si membrane reflectors with multilayer semiconductor NMs [146]. Waveguides using high performance SiNM on flexible substrates have also been demonstrated with low propagation loss of ~ 1.1 dB/cm [147]. With many of the integrated optics and photonics components prototypes built and tested using nanomembranes with compatible material systems (Figure 18), this technology holds the promise of practically realizing flexible photonic circuits [148, 149].

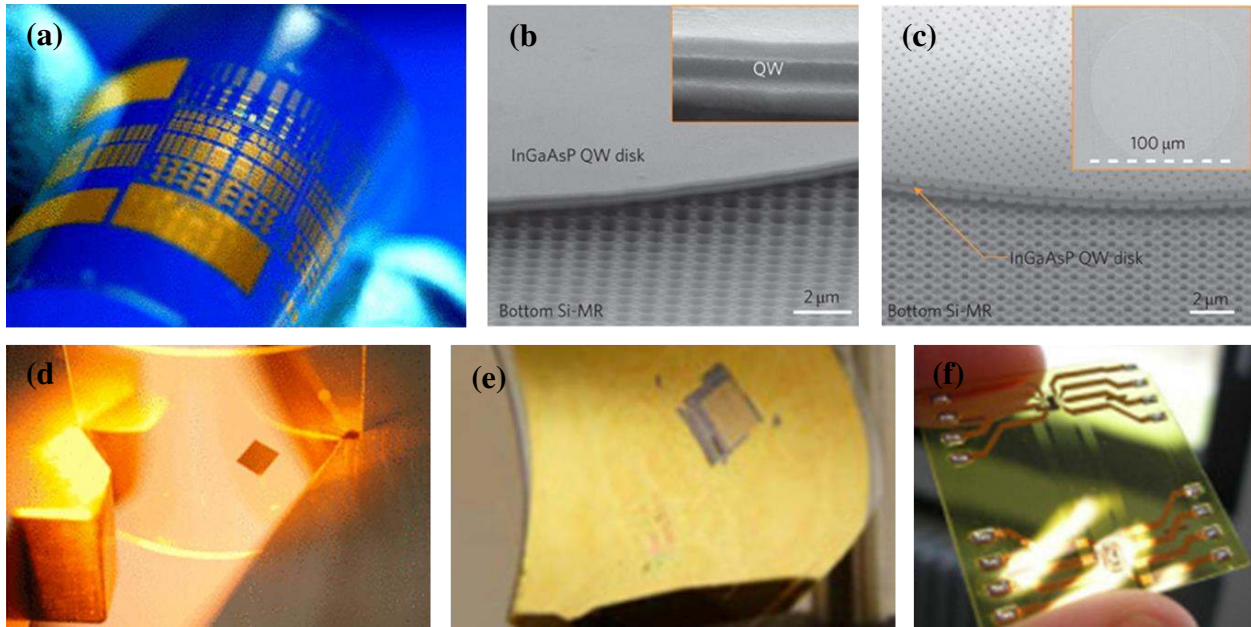


Figure 18: (a) Array of finished PIN diodes on a bent PET substrate [145], (b) and (c) shows transferred III-V InGaAsP quantum well heterostructure as the gain medium sandwiched between single layer Si photonic crystal membrane reflectors using multilayer stacked nanomembranes [146], (d) micrograph of 3x3 mm patterned nanomembrane transferred onto a 1x1" flexible PET substrate [148], (e) Image of fabricated photonic devices on Au coated PET substrate, (f) photo of a prototypical flexible optical link [149]

6. CONCLUSIONS

In this review, we have discussed the recent advances in the field of additive manufacturing as applied to EM structures, media and devices which have demonstrated the efficacy of using AM processes and methods to increase performance, add unique capabilities and also reduce time/cost when compared to traditional methods to fabricating these systems. The globalization of technology has increased the speed of innovation throughout the world. Ventures in the technical field, be it defense or industry, need to stay one step ahead of their competitors. This demands agile and rapid manufacturing and the enabling of open architectures that permit rapid prototyping tailored for specific applications, reconfigurability, efficient small lot productions, modularity, and complexity combined with flexibility as well as a shortened supply chain to enable better systems, faster and cheaper. Additive manufacturing and 3D prototyping is a

potential “game changer” and has important implications as seen by the significant investment by the Federal government through initiatives such as NNMI (America Makes). Rapid prototyping can provide the seamless thread from design to manufacturing to maintainability that will enable rapid modernization for technological agility. While AM technology has advanced considerably in the commercial sector for manufacturing with new materials like thermo-plastics, metals, and photopolymers, much work remains to be done to advance the use of these novel processes and materials to breakthrough applications that will allow rapid advancement of technical challenges from the factory to the laboratory environment.

7. ACKNOWLEDGMENTS

The authors are thankful for the funding support through the through AFOSR Lab Tasks 13RY02COR (AFOSR PO Dr. H. Weinstock) and 14RY07COR (PO: Dr. G. Pomrenke).

8. REFERENCES

- [1] K. Alexopoulos, N. Papakostas, D. Mourtzis, P. Gogos, and G. Chryssolouris, "Quantifying the flexibility of a manufacturing system by applying the transfer function," *Int. J. Comput. Integr. Manuf.*, vol. 20, pp. 538-547, 2007.
- [2] S. Hockfield, A. Liveris, R. Birgeneau, W. G. Bush, L. Chenevert, J. Cohon, *et al.*, "Report to the President on Capturing Domestic Competitive Advantage in Advanced Manufacturing," President's Council of Advisors on Science and Technology 2012.
- [3] O. Ivanova, C. Williams, and T. Campbell, "Additive manufacturing (AM) and nanotechnology: promises and challenges," *Rapid Prototyping Journal*, vol. 19, pp. 353-364, 2013.
- [4] S. M. Mikki and A. A. Kishk, "Electromagnetic wave propagation in nonlocal media: negative group velocity and beyond," *Progress In Electromagnetics Research B*, vol. 14, pp. 149-174, 2009.
- [5] Y. Liu and X. Zhang, "Metamaterials: a new frontier of science and technology," *Chemical Society Reviews*, vol. 40, pp. 2494-2507, 2011.
- [6] C. L. Peterson, "Nanotechnology: from Feynman to the grand challenge of molecular manufacturing," *Technology and Society Magazine, IEEE*, vol. 23, pp. 9-15, 2004.
- [7] M. Lapine and S. Tretyakov, "Contemporary notes on metamaterials," *Microwaves, Antennas & Propagation, IET*, vol. 1, pp. 3-11, 2007.
- [8] C. R. Garcia, J. Correa, D. Espalin, J. H. Barton, R. C. Rumpf, R. Wicker, *et al.*, "3D printing of anisotropic metamaterials," *Progress In Electromagnetics Research Letters*, vol. 34, pp. 75-82, 2012.
- [9] B. J. Willis, "Compact form fitting small antennas using three-dimensional rapid prototyping," Doctor of Philosophy, Department of Electrical and Computer Engineering, The University of Utah, 2012.
- [10] L. J. Chu, "Physical Limitations of Omni-Directional Antennas," *Journal of Applied Physics*, vol. 19, pp. 1163-1175, 1948.
- [11] H. A. Wheeler, "Small antennas," *Antennas and Propagation, IEEE Transactions on*, vol. 23, pp. 462-469, 1975.
- [12] R. F. Harrington, "Effects of antenna size on gain, bandwidth, and efficiency," *Journal of National Bureau of Standards*, vol. 64, pp. 1-12, 1960.
- [13] H. L. Thal, "New Radiation Q Limits for Spherical Wire Antennas," *Antennas and Propagation, IEEE Transactions on*, vol. 54, pp. 2757-2763, 2006.

- [14] H. Mosallaei, "Complex Layered Materials and Periodic Electromagnetic Band-Gap Structures: Concepts, Characterizations, and Applications," Doctor of Philosophy, Electrical Engineering, University of California, Los Angeles, 2001.
- [15] P. de Maagt, R. Gonzalo, Y. C. Vardaxoglou, and J. M. Baracco, "Electromagnetic bandgap antennas and components for microwave and (Sub)millimeter wave applications," *Antennas and Propagation, IEEE Transactions on*, vol. 51, pp. 2667-2677, 2003.
- [16] R. C. Rumpf, J. Pazos, C. R. Garcia, L. Ochoa, and R. Wicker, "3D Printed Lattices with Spatially Variant Self-Collimation," *Progress In Electromagnetics Research*, vol. 139, pp. 1-14, 2013.
- [17] R. M. Walser, "Electromagnetic metamaterials," 2001, pp. 1-15.
- [18] P. I. Deffenbaugh, "3D printed electromagnetic transmission and electronic structures fabricated on a single platform using advanced process integration techniques," Ph.D, Electrical engineering, The University of Texas at El Paso, 2014.
- [19] A. Sihvola, "Electromagnetic Emergence in Metamaterials," in *Advances in Electromagnetics of Complex Media and Metamaterials*. vol. 89, S. Zouhdi, A. Sihvola, and M. Arsalane, Eds., ed: Springer Netherlands, 2002, pp. 3-17.
- [20] J. Valentine, S. Zhang, T. Zentgraf, E. Ulin-Avila, D. A. Genov, G. Bartal, *et al.*, "Three-dimensional optical metamaterial with a negative refractive index," *Nature*, vol. 455, pp. 376-379, 2008.
- [21] Z. Jiang, M. Stickel, and G. V. Eleftheriades, "A broadband negative-refractive-index transmission-line (NRI-TL) stacked metamaterial for incident plane waves," in *Antennas and Propagation Society International Symposium, 2007 IEEE*, 2007, pp. 2357-2360.
- [22] D. Chanda, K. Shigeta, S. Gupta, T. Cain, A. Carlson, A. Mihi, *et al.*, "Large-area flexible 3D optical negative index metamaterial formed by nanotransfer printing," *Nat Nano*, vol. 6, pp. 402-407, 2011.
- [23] M. LaMonica. (2013). *10 breakthrough technologies: Additive manufacturing* (<http://www.technologyreview.com/featuredstory/513716/additive-manufacturing/> ed.).
- [24] D. T. Pham and R. S. Gault, "A comparison of rapid prototyping technologies," *International Journal of Machine Tools and Manufacture*, vol. 38, pp. 1257-1287, 1998.
- [25] J. S. Shirk, M. Sandrock, D. Scribner, E. Fleet, R. Stroman, E. Baer, *et al.*, "Biomimetic Gradient Index (GRIN) Lenses," *NRL REVIEW*, pp. 53-61, 2006.
- [26] T. Driscoll, D. N. Basov, A. F. Starr, P. M. Rye, S. Nemat-Nasser, D. Schurig, *et al.*, "Free-space microwave focusing by a negative-index gradient lens," *Applied Physics Letters*, vol. 88, p. 081101, 2006.
- [27] M. Hui Feng, C. Ben Geng, Z. Teng Xiang, Y. Yan, J. Wei Xiang, and C. Tie Jun, "Three-Dimensional Gradient-Index Materials and Their Applications in Microwave Lens Antennas," *Antennas and Propagation, IEEE Transactions on*, vol. 61, pp. 2561-2569, 2013.
- [28] N. C. Evans and D. L. Shealy, "Design of a gradient-index beam shaping system via a genetic algorithm optimization method," 2000, pp. 26-39.
- [29] J. W. Allen and B. I. Wu, "Design and fabrication of an RF GRIN lens using 3D printing technology," 2013, pp. 86240V-86240V-7.
- [30] F.-Y. Meng, R.-Z. Liu, K. Zhang, D. Erni, Q. Wu, L. Sun, *et al.*, "Automatic design of broadband gradient index metamaterial lens for gain enhancement of circularly polarized antennas," *Progress In Electromagnetics Research Letters*, vol. 141, pp. 17-32, 2013.
- [31] Y. L. Kong, I. A. Tamargo, H. Kim, B. N. Johnson, M. K. Gupta, T.-W. Koh, *et al.*, "3D Printed Quantum Dot Light-Emitting Diodes," *Nano Letters*, vol. 14, pp. 7017-7023, 2014/12/10 2014.
- [32] M. S. Mannoor, Z. Jiang, T. James, Y. L. Kong, K. A. Malatesta, W. O. Soboyejo, *et al.*, "3D Printed Bionic Ears," *Nano Letters*, vol. 13, pp. 2634-2639, 2013/06/12 2013.

- [33] Y. Urzhumov, N. Landy, T. Driscoll, D. Basov, and D. R. Smith, "Thin low-loss dielectric coatings for free-space cloaking," *Optics Letters*, vol. 38, pp. 1606-1608, 2013/05/15 2013.
- [34] A. F. d. Baas, S. Tretyakov, P. Barois, T. Scharf, V. Kruglyak, and I. Bergmair. (2010). *Nanostructured Metamaterials: Exchange between experts in electromagnetics and material science*
- [35] A. V. Kildishev and V. M. Shalaev, "Transformation optics and metamaterials," *Physics-Uspekhi*, vol. 54, p. 53, 2011.
- [36] J. Allen, "Application of Metamaterials to the Optimization of Smart Antenna Systems ", Electrical and Computer Engineering, Duke University, Durham, 2011.
- [37] M. Wegener, "Photonic Metamaterials and Transformation Optics: A Very Brief Introduction and Review," ed: NATO Science for Peace and Security Series B: Physics and Biophysics, 2013.
- [38] M. Rahm, S. A. Cummer, D. Schurig, J. B. Pendry, and D. R. Smith, "Optical Design of Reflectionless Complex Media by Finite Embedded Coordinate Transformations," *Physical Review Letters*, vol. 100, p. 063903, 2008.
- [39] D. Schurig, J. B. Pendry, and D. R. Smith, "Transformation-designed optical elements," *Optics Express*, vol. 15, pp. 14772-14782, 2007/10/29 2007.
- [40] A. J. Ward and J. B. Pendry, "Refraction and geometry in Maxwell's equations," *Journal of Modern Optics*, vol. 43, pp. 773-793, 1996/04/01 1996.
- [41] J. B. Pendry, D. Schurig, and D. R. Smith, "Controlling Electromagnetic Fields," *Science*, vol. 312, pp. 1780-1782, June 23, 2006 2006.
- [42] M. Rahm, D. Schurig, D. A. Roberts, S. A. Cummer, D. R. Smith, and J. B. Pendry, "Design of electromagnetic cloaks and concentrators using form-invariant coordinate transformations of Maxwell's equations," *Photonics and Nanostructures - Fundamentals and Applications*, vol. 6, pp. 87-95, 2008.
- [43] J. Allen, N. Kundtz, D. A. Roberts, S. A. Cummer, and D. R. Smith, "Electromagnetic source transformations using superellipse equations," *Applied Physics Letters*, vol. 94, p. 194101, 2009.
- [44] J. W. Allen, H. Steyskal, and D. R. Smith, "Impedance and complex power of radiating elements under electromagnetic source transformation," *Microwave and Optical Technology Letters*, vol. 53, pp. 1524-1527, 2011.
- [45] N. Kundtz, D. A. Roberts, J. Allen, S. Cummer, and D. R. Smith, "Optical source transformations," *Optics Express*, vol. 16, pp. 21215-21222, 2008/12/22 2008.
- [46] B.-I. Popa and S. A. Cummer, "Cloaking with optimized homogeneous anisotropic layers," *Physical Review A*, vol. 79, p. 023806, 2009.
- [47] V. Topa, E. Simion, and C. Munteanu, "Optimization Techniques in the Design of Electromagnetic Devices," in *Electric and Magnetic Fields*, A. Nicolet and R. Belmans, Eds., ed: Springer US, 1995, pp. 189-192.
- [48] M. Mussetta, F. Grimaccia, and R. E. Zich, "Comparison of different optimization techniques in the design of electromagnetic devices," in *Evolutionary Computation (CEC), 2012 IEEE Congress on*, 2012, pp. 1-6.
- [49] J.-L. Lin, C.-H. Wu, and H.-Y. Chung, "Performance Comparison of Electromagnetism-Like Algorithms for Global Optimization," *Applied Mathematics*, vol. 3, pp. 1265-1275, 2012.
- [50] S. Xiao, M. Rotaru, and J. K. Sykulski. (2015). Correlation matrices in kriging assisted optimisation of electromagnetic devices. *IET Science, Measurement & Technology*. Available: <http://digital-library.theiet.org/content/journals/10.1049/iet-smt.2014.0194>
- [51] D. R. Smith, "Analytic expressions for the constitutive parameters of magnetoelectric metamaterials," *Physical Review E*, vol. 81, p. 036605, 2010.

- [52] C. Caloz and T. Itoh, "TL Theory of MTMs," in *Electromagnetic Metamaterials: Transmission Line Theory and Microwave Applications*, ed: John Wiley & Sons, Inc., 2005, pp. 59-132.
- [53] E. Pourtrina, H. Da, and R. S. David, "Analysis of nonlinear electromagnetic metamaterials," *New Journal of Physics*, vol. 12, p. 093010, 2010.
- [54] N. Lazarides and G. P. Tsironis, "Coupled nonlinear Schrodinger field equations for electromagnetic wave propagation in nonlinear left-handed materials," *Physical Review E*, vol. 71, p. 036614, 2005.
- [55] S. A. Tretyakov, S. Maslovski, and P. A. Belov, "An analytical model of metamaterials based on loaded wire dipoles," *Antennas and Propagation, IEEE Transactions on*, vol. 51, pp. 2652-2658, 2003.
- [56] (2013). <https://americamakes.us/index.php>.
- [57] K. D. D. Willis, E. Brockmeyer, S. Hudson, and I. Poupyrev, "Printed optics: 3D printing of embedded optical elements for interactive devices," in *Proceedings of the 25th annual ACM symposium on User interface software and technology*, Cambridge, MA, 2012.
- [58] B. Zhang, "Electrodynamics of transformation-based invisibility cloaking," *Light Sci Appl*, vol. 1, p. e32, 2012.
- [59] M. Bresin, N. Nehru, and J. T. Hastings, "Focused electron-beam induced deposition of plasmonic nanostructures from aqueous solutions," 2013, pp. 861306-861306-6.
- [60] R. DGA. (2013, Additive Vs subtractive manufacturing. *Rapid Prototyping Technology*, 50-54.
- [61] A. International, "ASTM F2792-12a, Standard Terminology for Additive Manufacturing Technologies," ed. West Conshohocken, PA: www.astm.org, 2012.
- [62] S. Meteyer, X. Xu, N. Perry, and Y. F. Zhao, "Energy and Material Flow Analysis of Binder-jetting Additive Manufacturing Processes," *Procedia CIRP*, vol. 15, pp. 19-25, 2014.
- [63] F. Liou, "Modeling and Its Applications to Metal Additive Manufacturing Processes," in *24th Advanced Aerospace Materials and Processes (AeroMat) Conference and Exposition*, 2013.
- [64] S. Upcraft and R. Fletcher, "The rapid prototyping technologies," *Assembly Automation*, vol. 23, pp. 318-330, 2003.
- [65] J.-U. Park, M. Hardy, S. J. Kang, K. Barton, K. Adair, D. k. Mukhopadhyay, *et al.*, "High-resolution electrohydrodynamic jet printing," *Nat Mater*, vol. 6, pp. 782-789, 2007.
- [66] I. Gibson, D. W. Rosen, and B. Stucker, "Powder Bed Fusion Processes," in *Additive Manufacturing Technologies*, ed: Springer US, 2010, pp. 120-159.
- [67] A. Boltasseva and V. M. Shalaev, "Fabrication of optical negative-index metamaterials: Recent advances and outlook," *Metamaterials*, vol. 2, pp. 1-17, 2008.
- [68] J. B. Pendry, "A Chiral Route to Negative Refraction," *Science*, vol. 306, pp. 1353-1355, November 19, 2004 2004.
- [69] M. Decker, M. Ruther, C. E. Kriegler, J. Zhou, C. M. Soukoulis, S. Linden, *et al.*, "Strong optical activity from twisted-cross photonic metamaterials," *Optics Letters*, vol. 34, pp. 2501-2503, 2009/08/15 2009.
- [70] E. Plum, V. A. Fedotov, A. S. Schwanecke, N. I. Zheludev, and Y. Chen, "Giant optical gyrotropy due to electromagnetic coupling," *Applied Physics Letters*, vol. 90, p. 223113, 2007.
- [71] M. Beruete, M. Navarro-Cía, M. Sorolla, and I. Campillo, "Planoconcave lens by negative refraction of stacked subwavelength hole arrays," *Optics Express*, vol. 16, pp. 9677-9683, 2008/06/23 2008.
- [72] C. M. Soukoulis, S. Linden, and M. Wegener, "Negative Refractive Index at Optical Wavelengths," *Science*, vol. 315, pp. 47-49, January 5, 2007 2007.
- [73] O. S. Kim. (2013, EMS group prints 3D antennas. *Denmark Technical University, Electrical Engineering News*.

- [74] C. M. Soukoulis and M. Wegener, "Past achievements and future challenges in the development of three-dimensional photonic metamaterials," *Nat Photon*, vol. 5, pp. 523-530, 2011.
- [75] T. J. Talty, D. Yingcheng, and L. Lanctot, "Automotive antennas: trends and future requirements," in *Antennas and Propagation Society International Symposium, 2001. IEEE*, 2001, pp. 430-433 vol.1.
- [76] S. Gao, K. Clark, M. Unwin, J. Zackrisson, W. A. Shiroma, J. M. Akagi, *et al.*, "Antennas for Modern Small Satellites," *Antennas and Propagation Magazine, IEEE*, vol. 51, pp. 40-56, 2009.
- [77] H. Morishita, K. Yongho, and K. Fujimoto, "Design concept of antennas for small mobile terminals and the future perspective," *Antennas and Propagation Magazine, IEEE*, vol. 44, pp. 30-43, 2002.
- [78] F. Namin and D. H. Werner, "Design of volumetric antenna arrays based on three-dimensional aperiodic tilings," in *Antennas and Propagation Society International Symposium (APSURSI), 2010 IEEE*, 2010, pp. 1-4.
- [79] A. Elsherbini and K. Sarabandi, "Very Low-Profile Top-Loaded UWB Coupled Sectorial Loops Antenna," *Antennas and Wireless Propagation Letters, IEEE*, vol. 10, pp. 800-803, 2011.
- [80] C. P. Baliarda, J. Soler-Castany, J. I. Ortigosa-Vallejo, and J. Anguera-Pros, "Miniature antenna having a volumetric structure," ed: Google Patents, 2013.
- [81] D. Ye, K. Chang, L. Ran, and H. Xin, "Microwave gain medium with negative refractive index," *Nat Commun*, vol. 5, 2014.
- [82] I. M. Ehrenberg, S. E. Sarma, and B.-I. Wu, "A three-dimensional self-supporting low loss microwave lens with a negative refractive index," *Journal of Applied Physics*, vol. 112, p. 073114, 2012.
- [83] L. Min, N. Wei-Ren, C. Kihun, M. E. Gehm, and X. Hao, "An X-band Luneburg Lens antenna fabricated by rapid prototyping technology," in *Microwave Symposium Digest (MTT), 2011 IEEE MTT-S International*, 2011, pp. 1-4.
- [84] L. G. BV. (2015). *Printoptical technology and the 3D printing of functional optics*.
- [85] D. Jang, L. R. Meza, F. Greer, and J. R. Greer, "Fabrication and deformation of three-dimensional hollow ceramic nanostructures," *Nat Mater*, vol. 12, pp. 893-898, 2013.
- [86] L. Serrano-Ramón, R. Córdoba, L. A. Rodríguez, C. Magén, E. Snoeck, C. Gatel, *et al.*, "Ultrasmall Functional Ferromagnetic Nanostructures Grown by Focused Electron-Beam-Induced Deposition," *ACS Nano*, vol. 5, pp. 7781-7787, 2011/10/25 2011.
- [87] J. Chen, H. Doumanidis, K. Lyons, J. Murday, and M. Roco, "Manufacturing at the Nanoscale," 2007.
- [88] J. H. Jang, C. K. Ullal, M. Maldovan, T. Gorishnyy, S. Kooi, C. Koh, *et al.*, "3D Micro- and Nanostructures via Interference Lithography," *Advanced Functional Materials*, vol. 17, pp. 3027-3041, 2007.
- [89] S. Vignolini, N. A. Yufa, P. S. Cunha, S. Guldin, I. Rushkin, M. Stefik, *et al.*, "A 3D Optical Metamaterial Made by Self-Assembly," *Advanced Materials*, vol. 24, pp. OP23-OP27, 2012.
- [90] K. A. Arpin, A. Mihi, H. T. Johnson, A. J. Baca, J. A. Rogers, J. A. Lewis, *et al.*, "Multidimensional Architectures for Functional Optical Devices," *Advanced Materials*, vol. 22, pp. 1084-1101, 2010.
- [91] G. M. Whitesides, J. K. Kriebel, and B. T. N. Mayers, Huck, , "Self-Assembly and Nanostructured Materials," in *anoscale Assembly: Chemical Techniques*. vol. VIII, ed: W.T.S., Eds., Springer (formerly Kluwer), 2005.
- [92] C. Liberale, G. Cojoc, P. Candeloro, G. Das, F. Gentile, F. De Angelis, *et al.*, "Micro-Optics Fabrication on Top of Optical Fibers Using Two-Photon Lithography," *Photonics Technology Letters, IEEE*, vol. 22, pp. 474-476, 2010.

- [93] C. Liberale, E. Fabrizio, G. Cojoc, G. Perozziello, P. Candeloro, F. Bragheri, *et al.*, "Optical fiber tweezers fabricated by two photon lithography," in *Lasers and Electro-Optics Europe (CLEO EUROPE/EQEC), 2011 Conference on and 12th European Quantum Electronics Conference*, 2011, pp. 1-1.
- [94] C. Liberale, P. Minzioni, F. Bragheri, F. De Angelis, E. Di Fabrizio, and I. Cristiani, "Miniaturized all-fibre probe for three-dimensional optical trapping and manipulation," *Nat Photon*, vol. 1, pp. 723-727, 2007.
- [95] S. Kawata, H.-B. Sun, T. Tanaka, and K. Takada, "Finer features for functional microdevices," *Nature*, vol. 412, pp. 697-698, 2001.
- [96] P. Calvert, "Inkjet Printing for Materials and Devices," *Chemistry of Materials*, vol. 13, pp. 3299-3305, 2001/10/01 2001.
- [97] M. Huth, F. Porrati, C. Schwalb, M. Winhold, R. Sachser, M. Dukic, *et al.*, "Focused electron beam induced deposition: A perspective," *Beilstein Journal of Nanotechnology*, vol. 3, pp. 597-619, 2012.
- [98] W. F. van Dorp and C. W. Hagen, "A critical literature review of focused electron beam induced deposition," *Journal of Applied Physics*, vol. 104, p. 081301, 2008.
- [99] S. Jeon, J.-U. Park, R. Cirelli, S. Yang, C. E. Heitzman, P. V. Braun, *et al.*, "Fabricating complex three-dimensional nanostructures with high-resolution conformable phase masks," *Proceedings of the National Academy of Sciences of the United States of America*, vol. 101, pp. 12428-12433, August 24, 2004 2004.
- [100] J. D. Joannopoulos, P. R. Villeneuve, and S. Fan, "Photonic crystals: putting a new twist on light," *Nature*, vol. 386, pp. 143-149, 1997.
- [101] R. H. Lipson and C. Lu, "Photonic crystals: a unique partnership between light and matter," *European Journal of Physics*, vol. 30, p. S33, 2009.
- [102] D. Shir, E. C. Nelson, Y. C. Chen, A. Brzezinski, H. Liao, P. V. Braun, *et al.*, "Three dimensional silicon photonic crystals fabricated by two photon phase mask lithography," *Applied Physics Letters*, vol. 94, p. 011101, 2009.
- [103] V. Mizeikis, K. K. Seet, S. Juodkakis, V. Jarutis, and H. Misawa, "Two-Photon Laser Lithography of photonic microstructures in photoresist SU-8," in *Lasers and Electro-Optics, 2005. CLEO/Pacific Rim 2005. Pacific Rim Conference on*, 2005, pp. 1735-1736.
- [104] J. H. Atwater, P. Spinelli, E. Kosten, J. Parsons, C. Van Lare, J. Van de Groep, *et al.*, "Microphotonic parabolic light directors fabricated by two-photon lithography," *Applied Physics Letters*, vol. 99, p. 151113, 2011.
- [105] S. Jeon, V. Malyarchuk, J. A. Rogers, and G. P. Wiederrecht, "Fabricating three-dimensional nanostructures using two photon lithography in a single exposure step," *Optics Express*, vol. 14, pp. 2300-2308, 2006/03/20 2006.
- [106] P. Jinsoon, Y. Byeongil, K. Ran Hee, C. Namchul, and L. Kwang-Sup, "Recent Advances in Three Dimensional Microfabrications by Two-Photon Lithography," in *Lasers and Electro-Optics Society, 2007. LEOS 2007. The 20th Annual Meeting of the IEEE*, 2007, pp. 749-750.
- [107] E.-H. Kil, K.-H. Choi, H.-J. Ha, S. Xu, J. A. Rogers, M. R. Kim, *et al.*, "Imprintable, Bendable, and Shape-Conformable Polymer Electrolytes for Versatile-Shaped Lithium-Ion Batteries," *Advanced Materials*, vol. 25, pp. 1395-1400, 2013.
- [108] E. Menard, L. Bilhaut, J. Zaumseil, and J. A. Rogers, "Improved Surface Chemistries, Thin Film Deposition Techniques, and Stamp Designs for Nanotransfer Printing," *Langmuir*, vol. 20, pp. 6871-6878, 2004/08/01 2004.

- [109] A. Perentes, A. Bachmann, M. Leutenegger, I. Utke, C. Sandu, and P. Hoffmann, "Focused electron beam induced deposition of a periodic transparent nano-optic pattern," *Microelectronic Engineering*, vol. 73–74, pp. 412-416, 2004.
- [110] K. Ohlinger, F. Torres, Y. Lin, K. Lozano, D. Xu, and K. P. Chen, "Photonic crystals with defect structures fabricated through a combination of holographic lithography and two-photon lithography," *Journal of Applied Physics*, vol. 108, p. 073113, 2010.
- [111] S. M. Kuebler, K. L. Braun, F. Stellacci, C. A. Bauer, M. Halik, Z. Wenhui, *et al.*, "Two-photon 3D lithography: materials and applications," in *Lasers and Electro-Optics Society, 2004. LEOS 2004. The 17th Annual Meeting of the IEEE, 2004*, pp. 561-562 Vol.2.
- [112] A. Dhawan, M. Gerhold, A. Madison, J. Fowlkes, P. E. Russell, T. Vo-Dinh, *et al.*, "Fabrication of nanodot plasmonic waveguide structures using FIB milling and electron beam-induced deposition," *Scanning*, vol. 31, pp. 139-146, 2009.
- [113] P. Galliker, J. Schneider, H. Eghlidi, S. Kress, V. Sandoghdar, and D. Poulikakos, "Direct printing of nanostructures by electrostatic autofocussing of ink nanodroplets," *Nat Commun*, vol. 3, p. 890, 2012.
- [114] A. Fernández-Pacheco, L. Serrano-Ramón, J. M. Michalik, M. R. Ibarra, J. M. De Teresa, L. O'Brien, *et al.*, "Three dimensional magnetic nanowires grown by focused electron-beam induced deposition," *Sci. Rep.*, vol. 3, 2013.
- [115] S. Ushiba, S. Shoji, K. Masui, P. Kuray, J. Kono, and S. Kawata, "3D microfabrication of single-wall carbon nanotube/polymer composites by two-photon polymerization lithography," *Carbon*, vol. 59, pp. 283-288, 2013.
- [116] J. K. Gansel, M. Thiel, M. S. Rill, M. Decker, K. Bade, V. Saile, *et al.*, "Gold Helix Photonic Metamaterial as Broadband Circular Polarizer," *Science*, vol. 325, pp. 1513-1515, September 18, 2009 2009.
- [117] C. Helgert, "Symmetry-related effects of optical metamaterials," Physikalisch-Astronomischen Fakultät, Friedrich-Schiller-Universität Jena, 2011.
- [118] P. Pa, M. S. Mirotznik, R. McCauley, S. Yarlagadda, and K. Duncan, "Integrating metamaterials within a structural composite using additive manufacturing methods," in *Antennas and Propagation Society International Symposium (APSURSI), 2012 IEEE, 2012*, pp. 1-2.
- [119] H. Teguh Yudistira, A. Pradhipta Tenggara, V. Dat Nguyen, T. Teun Kim, F. Dian Prasetyo, C.-g. Choi, *et al.*, "Fabrication of terahertz metamaterial with high refractive index using high-resolution electrohydrodynamic jet printing," *Applied Physics Letters*, vol. 103, p. 211106, 2013.
- [120] M. S. Rill, C. E. Kriegler, M. Thiel, G. von Freymann, S. Linden, and M. Wegener, "Negative-index bianisotropic photonic metamaterial fabricated by direct laser writing and silver shadow evaporation," *Optics Letters*, vol. 34, pp. 19-21, 2009/01/01 2009.
- [121] X. Xiong, Z.-H. Xue, C. Meng, S.-C. Jiang, Y.-H. Hu, R.-W. Peng, *et al.*, "Polarization-dependent perfect absorbers/reflectors based on a three-dimensional metamaterial," *Physical Review B*, vol. 88, p. 115105, 2013.
- [122] S. Maruo. (2012, 3D molding processes based on two-photon microfabrication. *SPIE Newsroom*.
- [123] S. Maruo and J. T. Fourkas, "Recent progress in multiphoton microfabrication," *Laser & Photonics Reviews*, vol. 2, pp. 100-111, 2008.
- [124] S. Maruo, O. Nakamura, and S. Kawata, "Three-dimensional microfabrication with two-photon-absorbed photopolymerization," *Optics Letters*, vol. 22, pp. 132-134, 1997/01/15 1997.
- [125] H. Schippers, G. Vos, and H. van Tongeren, "Aerodynamic, structural and electromagnetic interaction applied to conformal antennas," in *Analysis and Simulation of Multifield Problems*. vol. 12, W. Wendland and M. Efendiev, Eds., ed: Springer Berlin Heidelberg, 2003, pp. 329-336.

- [126] S. R. Pine, "Manufacturing structurally integrated three dimensional phased array antennas," Master of Science, Mechanical Engineering, Georgia Institute of Technology, 2006.
- [127] K. Ghorbani, "Conformal load bearing antenna structure using Carbon Fibre Reinforced Polymer (CFRP)," in *Antenna Technology: "Small Antennas, Novel EM Structures and Materials, and Applications" (iWAT), 2014 International Workshop on*, 2014, pp. 118-118.
- [128] R. Poisel, *Antenna Systems and Electronic Warfare Applications* Artech House, 2012.
- [129] L. Josefsson and P. Persson, *Conformal array antenna theory and design*: John Wiley & Sons, Inc, 2006.
- [130] P. Knott, "Design of a triple patch antenna element for double curved conformal antenna arrays," in *Antennas and Propagation, 2006. EuCAP 2006. First European Conference on*, 2006, pp. 1-4.
- [131] D. B. Burckel, J. R. Wendt, G. A. Ten Eyck, A. R. Ellis, I. Brener, and M. B. Sinclair, "Fabrication of 3D Metamaterial Resonators Using Self-Aligned Membrane Projection Lithography," *Advanced Materials*, vol. 22, pp. 3171-3175, 2010.
- [132] J. G. Kim, N. Takama, B. J. Kim, and H. Fujita, "Optical-softlithographic technology for patterning on curved surfaces," *Journal of Micromechanics and Microengineering*, vol. 19, p. 055017, 2009.
- [133] D. J. Gregoire, "3D artificial impedance surfaces," in *Antennas and Propagation Society International Symposium (APSURSI), 2012 IEEE*, 2012, pp. 1-2.
- [134] J. J. Adams, S. C. Slimmer, T. F. Malkowski, E. B. Duoss, J. A. Lewis, and J. T. Bernhard, "Comparison of Spherical Antennas Fabricated via Conformal Printing: Helix, Meanderline, and Hybrid Designs," *Antennas and Wireless Propagation Letters, IEEE*, vol. 10, pp. 1425-1428, 2011.
- [135] J. J. Adams, E. B. Duoss, T. F. Malkowski, M. J. Motala, B. Y. Ahn, R. G. Nuzzo, *et al.*, "Conformal Printing of Electrically Small Antennas on Three-Dimensional Surfaces," *Advanced Materials*, vol. 23, pp. 1335-1340, 2011.
- [136] J. J. Adams, E. B. Duoss, T. F. Malkowski, J. A. Lewis, and J. T. Bernhard, "Design of spherical meanderline antennas," in *Antennas and Propagation (APSURSI), 2011 IEEE International Symposium on*, 2011, pp. 765-768.
- [137] I. M. Ehrenberg, S. E. Sarma, and B. Wu, "Fully conformal FSS via rapid 3D prototyping," in *Antennas and Propagation Society International Symposium (APSURSI), 2012 IEEE*, 2012, pp. 1-2.
- [138] B. I. Wu and I. Ehrenberg, "Ultra conformal patch antenna array on a doubly curved surface," in *Phased Array Systems & Technology, 2013 IEEE International Symposium on*, 2013, pp. 792-798.
- [139] S. R. Best, "The radiation properties of electrically small folded spherical helix antennas," *Antennas and Propagation, IEEE Transactions on*, vol. 52, pp. 953-960, 2004.
- [140] C. B. Ravipati and S. R. Best, "The goubau multi element monopole antenna - revisited," in *Antennas and Propagation Society International Symposium, 2007 IEEE*, 2007, pp. 233-236.
- [141] P. Nga Phuong, E. Boellaard, J. N. Burghartz, and P. M. Sarro, "Photoresist coating methods for the integration of novel 3-D RF microstructures," *Microelectromechanical Systems, Journal of*, vol. 13, pp. 491-499, 2004.
- [142] R. Chen, "Three Dimensionally Interconnected Silicon Nanomembranes for Optical Phased Array (OPA) and Optical True Time Delay (TTD) Applications " University of Texas, Austin 2012.
- [143] J. A. Rogers, M. G. Lagally, and R. G. Nuzzo, "Synthesis, assembly and applications of semiconductor nanomembranes," *Nature*, vol. 477, pp. 45-53, 2011.
- [144] Z. Weidong and M. Zhenqiang, "Breakthroughs in Photonics 2012: Breakthroughs in Nanomembranes and Nanomembrane Lasers," *Photonics Journal, IEEE*, vol. 5, pp. 0700707-0700707, 2013.

- [145] H.-C. Yuan, J. Shin, G. Qin, L. Sun, P. Bhattacharya, M. G. Lagally, *et al.*, "Flexible photodetectors on plastic substrates by use of printing transferred single-crystal germanium membranes," *Applied Physics Letters*, vol. 94, p. 013102, 2009.
- [146] H. Yang, D. Zhao, S. Chuwongin, J.-H. Seo, W. Yang, Y. Shuai, *et al.*, "Transfer-printed stacked nanomembrane lasers on silicon," *Nat Photon*, vol. 6, pp. 615-620, 2012.
- [147] X. Xiaochuan, H. Subbaraman, A. Hosseini, D. Kwong, L. Che-Yun, and R. T. Chen, "Stamp printing of silicon nanomembrane based flexible photonic devices," in *Lasers and Electro-Optics (CLEO), 2012 Conference on, 2012*, pp. 1-2.
- [148] Z. Weidong, M. Zhenqiang, Y. Weiquan, S. Chuwongin, S. Yi-Chen, S. Jung-Hun, *et al.*, "Semiconductor nanomembranes for integrated and flexible photonics," in *Information Photonics (IP), 2011 ICO International Conference on, 2011*, pp. 1-2.
- [149] J. Hu, L. Li, H. Lin, P. Zhang, W. Zhou, and Z. Ma, "Flexible integrated photonics: where materials, mechanics and optics meet [Invited]," *Optical Materials Express*, vol. 3, pp. 1313-1331, 2013/09/01 2013.